Molecular Biology of the Cell
Vol. 18, 4669–4680, November 2007

Amphiphysin 1 Is Important for Actin Polymerization during Phagocytosis[D]

Hiroshi Yamada,* Emiko Ohashi,* Tadashi Abe,* Norihiro Kusumi,† Shun-AI Li,* Yumi Yoshida,* Masami Watanabe,† Kazuhito Tomizawa,‡ Yuji Kashiwakura,§ Hiromi Kumon,† Hideki Matsui,‡ and Kohji Takei*

Departments of *Neuroscience, †Urology and ‡Cell Physiology, Okayama University Graduate School of Medicine, Dentistry and Pharmaceutical Sciences, Okayama 700-8558, Japan; and §Innovation Center Okayama for Nanobio-Targeted Therapy, Graduate School of Medicine, Dentistry and Pharmaceutical Sciences, Okayama University, Okayama 700-8558, Japan

Submitted April 2, 2007; Revised August 21, 2007; Accepted August 30, 2007
Monitoring Editor: David Drubin

Amphiphysin 1 is involved in clathrin-mediated endocytosis. In this study, we demonstrate that amphiphysin 1 is essential for cellular phagocytosis and that it is critical for actin polymerization. Phagocytosis in Sertoli cells was induced by stimulating phosphatidylserine receptors. This stimulation led to the formation of actin-rich structures, including ruffles, phagocytic cups, and phagosomes, all of which showed an accumulation of amphiphysin 1. Knocking out amphiphysin 1 by RNA interference in the cells resulted in the reduction of ruffle formation, actin polymerization, and phagocytosis. Phagocytosis was also drastically decreased in amph 1 (−/−) Sertoli cells. In addition, phosphatidylinositol-4,5-bisphosphate–induced actin polymerization was decreased in the knockout testis cytosol. The addition of recombinant amphiphysin 1 to the cytosol restored the polymerization process. Ruffle formation in small interfering RNA-treated cells was recovered by the expression of constitutively active Rac1, suggesting that amphiphysin 1 functions upstream of the protein. These findings support that amphiphysin 1 is important in the regulation of actin dynamics and that it is required for phagocytosis.

INTRODUCTION

Phagocytosis is a form of endocytosis in which large molecules are engulfed by the plasma membrane and internalized for digestion (Greenberg and Grinstein, 2002; Niedergang and Chavrier, 2004). In vertebrates, macrophages and testicular Sertoli cells are the predominant phagocytes. Phagocytosis contributes to removal of foreign bodies, bacteria, and microbe-infected and apoptotic cells. Binding of these objects to the receptors, such as Fcγ receptors or phosphatidylserine receptors, on the surface of the macrophage initiates membrane remodeling and reorganization of the actin cytoskeleton. Cytoskeletal changes cause the cells to extend pseudopods that then engulf the objects (Anderem and Underhill, 1999).

Sertoli cells participate in the maturation of germ cells and the release of sperm (Russell *et al.*, 1990). These cells are highly phagocytic and are responsible for eliminating the residual cytoplasm of spermatids (Chemes, 1986; Clermont *et al.*, 1987; Morales and Clermont, 1991). The phagocytosis is also used to remove apoptotic germ cells (Shiratsuchi *et al.*, 1997, 1999; Kawasaki *et al.*, 2002). Phagocytosis in Sertoli cells is initiated by the recognition of phosphatidylserine (PS) found on the germ cell surface by PS receptors (Shiratsuchi *et al.*, 1997, 1999; Blanco-Rodriguez and Martinez-Garcia, 1999; Kawasaki *et al.*, 2002). The class B scavenger family receptors SR-BI and CD36 are found on the surface of Sertoli cells where they function in PS recognition (Shiratsuchi *et al.*, 1997, 1999; Kawasaki *et al.*, 2002; Gillot *et al.*, 2005). In the testis, Sertoli cells express high levels of amphiphysin 1 (Watanabe *et al.*, 2001; Kamitani *et al.*, 2002). The expression of amphiphysin, along with that of dynamin 2, increases with sexual development (Watanabe *et al.*, 2001); thus, it is hypothesized that amphiphysin 1 may play a role in spermatogenesis.

Amphiphysin 1 is found mainly in the neuronal synapse and in the testis. In the synapse, amphiphysin 1 acts as a linker between clathrin-coated proteins and dynamin 1 to assist in clathrin-mediated endocytosis (Slepnev *et al.*, 2000). Amphiphysin 1 and dynamin 1 are physiological binding partners, and they play a major role in the fission process of clathrin-mediated endocytosis (Schmid *et al.*, 1998; Takei *et al.*, 1999). Amphiphysin 1 has three functional domains, a highly conserved amino-terminal region composed of ~250 amino acids called the Bin/amphiphysin/Rvs (BAR) domain, a carboxy-terminal Src homology (SH)3 domain that binds dynamin 1 (David *et al.*, 1996; Wigge and McMahon, 1998), and clathrin/AP-2-binding sites (CLAP) at the central variable region (Slepnev *et al.*, 2000).

The BAR domain of amphiphysin 1 is a banana-shaped α-helical dimer that senses highly curved membranes (Peter *et al.*, 2004). It also contains an amphipathic helix at the amino terminus called N-BAR, which associates primarily with acidic phospholipids (Dawson *et al.*, 2006). This property enables the N-BAR proteins to induce membrane de-

This article was published online ahead of print in *MBC in Press* (http://www.molbiolcell.org/cgi/doi/10.1091/mbc.E07-04-0296) on September 12, 2007.

[D] The online version of this article contains supplemental material at *MBC Online* (http://www.molbiolcell.org).

Address correspondence to: Kohji Takei (kohji@md.okayama-u.ac.jp).

formation. It has recently been reported that N-BAR–containing proteins, such as the *Drosophila* amphiphysin isoform or endophilin function as a linker between the plasma membrane and the actin cytoskeleton (Dawson *et al.*, 2006). Phagocytosis requires actin dynamics; the actin polymerization underneath plasma membrane is thought to generate the driving forces of pushing (extension) or pulling (invagination) of the plasma membrane through a linker protein (Small *et al.*, 2002; Dawson *et al.*, 2006; Smythe and Ayscouh, 2006).

Amphiphysin has been previously interrelated with the actin cytoskeleton. Yeast amphiphysin isoforms Rvs 167 and Rvs 161 are involved in two actin-dependent processes, cellular polarity, and endocytosis (Munn *et al.*, 1995; Sivadon *et al.*, 1995; Kaksonen *et al.*, 2005). In neurons, amphiphysin 1 is colocalized with dynamin 1 at the filopodia formed in growth cones. The suppression of amphiphysin 1 by antisense oligonucleotides in the neurons decreases filopodia formation and leads to the collapse of the growth cones (Mundigl *et al.*, 1998; Yoo *et al.*, 2002). In the mature synapse, amphiphysin 1 localizes in proximity to actin cytomatrix (Bauerfeind *et al.*, 1997); however, the precise role of amphiphysin in actin dynamics is still not defined.

In this study, we analyze the function of amphiphysin 1 in actin dynamics during phagocytosis in Sertoli cells. We demonstrate a novel function for amphiphysin in the stimulation of actin polymerization in phagocytosis.

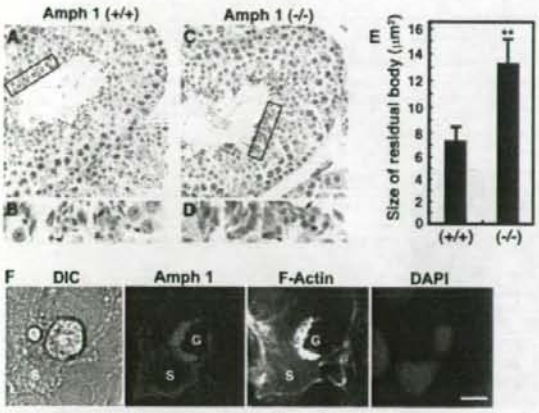

Figure 1. Amphiphysin 1 is implicated in phagocytosis in Sertoli cells. Hematoxylin- and eosin-stained low magnification images of seminiferous tubules at stage VIII in amph 1 (+/+) (A) or amph 1 (−/−) (C). Area enclosed with rectangles are shown at high magnification A and C (B and D, respectively). Arrowheads indicate residual bodies. Arrows indicate nuclei of spermatids. Note the difference in size in the wild type versus the mutant. Bar, 40 μm (A and C) and 10 μm (B and D). (E) Morphological analysis of residual bodies in size (area). The average area of the residual bodies in amph 1 (−/−) is ~1.8 times of that in wild type. Statistical significance was determined by Student's *t* tests (**$p < 0.01$, n = 200). (F) Primary rat cultured Sertoli cells (1×10^4 cells/coverslip) were incubated at 32°C for 30 min with germ cells (1×10^3 cells/coverslip) pretreated with camptothecin. The cells were fixed, permeabilized and stained with anti-amphiphysin 1 antibodies (mab 3) and Alexa488-phalloidin. Nuclei of the cells were visualized with DAPI. The Sertoli cells engulfed the apoptotic germ cells, whereas amphiphysin 1 accumulated at the phagocytic cup. G, germ cell; S, Sertoli cell. Bar, 10 μm.

MATERIALS AND METHODS

Animals

Three-week-old male Wister rats, 3-wk-old and 20-wk-old wild-type mice were purchased from Shimizu Laboratory Supplies Co. (Kyoto, Japan). Amphiphysin 1 knockout mice [amph 1 (−/−)] were generated by gene targeting in embryonic stem cells as described previously (Di Paolo *et al.*, 2002). Twenty-

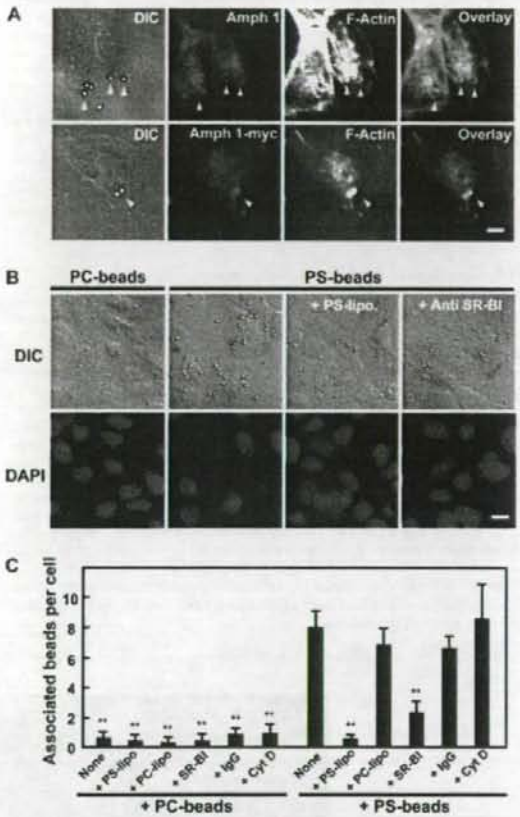

Figure 2. PS-dependent phagocytosis in Sertoli cells. (A) Amphiphysin 1 accumulates at phagosomes. Ser-W3 cells were transfected with amphiphysin 1-myc. After 24 h of transfection, the transfected cells were incubated with PS beads at 37°C for 90 min. They were fixed, permeabilized with digitonin, and stained with anti-amphiphysin 1 antibodies (mab 3) (top) and anti-myc antibodies (bottom) and Alexa488-phalloidin. Arrowheads indicate the incorporated beads surrounded by amphiphysin 1 and polymerized actin. Bar, 5 μm. (B and C) The association of beads with the Ser-W3 cells is PS and SR-BI dependent. Cells (1×10^4 cells on coverslips) were pretreated with 0.25 mM liposomes containing PS or PC at 37°C for 10 min. Then, cells were incubated in presence of beads coated with PS- or PC-liposomes at 37°C for 180 min. The cells were then washed, fixed, stained with DAPI, and analyzed by phase contrast microscopy. To block the binding of PS receptors to PS beads, cells were pretreated with anti-SR-BI antibodies or rabbit IgG as negative control at 100 μg/ml for 30 min (B). Bar, 10 μm. The number of beads associated with the cells was determined using phase contrast microscopy, and it is presented as the number of the beads per cell. To block the internalization, cells were pretreated with Cyt D at 2 μM for 30 min, and attached beads to the cells were analyzed. One hundred cells in 10 independent fields were counted in each experiment. All results are the mean ± SEM from three experiments. Statistical significance was determined by Student's *t* tests (**$p < 0.01$) (C).

week-old wild-type or amph 1 (−/−) mice were used for harvest of cytosol and hematoxyline-eosin staining, and 2–3-wk-old mice were used for primary culture. All animals were maintained in clean conditions with free access to food and water. They were allowed to adapt to their environment for more than 1 wk before initiating the experiments.

Cell Culture

Preparation of Sertoli cells and spermatogenetic cells from 3-wk-old rats or mice was done as described previously (Shiratsuchi *et al.*, 1997). Cells were cultured at 32°C under 5% CO_2. Mixture of Sertoli cells and germ cells were plated on collagen-coated culture dishes. After 24 h, the residual germ cells were removed by hypo-osmotic shock in 20 mM Tris-HCl, pH 7.4, for 3 min at room temperature. After 2 d of culture, the Sertoli cell-enriched culture consisted of ~95% Sertoli cells as established by immunofluorescent methods for the cell markers, Mullerian hormone, or amphiphysin 1 (Tran *et al.*, 1987; Watanabe *et al.*, 2001). Cells were plated in monolayers and experiments were performed. Ser-W3 cells were cultured with DMEM containing 10% fetal bovine serum at 37°C under 5% CO_2 (Prognan *et al.*, 1997). Apoptosis of the germ cells were induced by treatment with 2 μM camptothecin at 37°C for 8 h. Apoptosis was determined by analysis of fluorescein isothiocyanate (FITC)-annexin binding or chromatin condensation with 4,6-diamidino-2-phenylindole (DAPI) staining (Zhang *et al.*, 1998).

cDNA Constructs and Transfection

The cDNAs encoding full-length human amphiphysin 1 and its truncation constructs were prepared by polymerase chain reaction (PCR) amplification by using specific primers (Yoshida *et al.*, 2004). Full-length amphiphysin 1, amph 1-626aa (ΔSH3), and 226-695aa (ΔBAR) were subcloned into the plasmid pEF-BOS-myc or pGEX-6P vector as BamHI–EcoRI fragments. To prepare amph D322-386aa (ΔCLAP), amph D1-321aa was subcloned into a pGEX-6P vector as a BamHI–EcoRI fragment. EcoRI-EcoRI fragments containing amph 387-695aa were then inserted into the EcoRI site. Amph D322-386aa (ΔCLAP) was subcloned into a pEF-BOS-myc vector as BamHI–EcoRI fragments. Full-length amphiphysin 1 containing the BamHI and EcoRI restriction sites was subcloned into a pEGFP-C1 vector (Clontech, Mountain View, CA). The nucleotide sequences of the constructs were verified using DNA sequence analysis. The plasmids pEF-BOS-myc-N17Rac1, V12Rac1, N17Cdc42, and N17Rho were a gift from Dr. Toshiki Itoh (Kobe University, Japan). The constructs were transfected into the cells using a Lipofectamine 2000 transfection system (Invitrogen, Carlsbad, CA). The efficiency of transfection was ~90% in Ser-W3 cells determined by the levels of green fluorescence protein (GFP) expressed in the cells. Twenty-four hours after transfection, cells were subjected to phagocytic analysis.

Preparation for Liposomes and Lipid-coated Beads

Liposomes containing 70% phosphatidylcholine (PC) and 30% phosphatidylserine (PS) were prepared as described previously (Shiratsuchi *et al.*, 1997). For the actin polymerization assay, liposomes containing 46% PC, 30% PS, 20% cholesterol, 4% phosphatidylinositol-4,5-bisphosphate [PI(4,5)P_2] were prepared by sonication as described in Ma *et al.* (1998b). To prepare the PS-coated styrene beads, liposomes composed of 30% PS, 60% PC, and 10% biotinylated phosphatidylethanolamine (PE) (Invitrogen) were first made by sonication in serum-free DMEM. Two milligrams of the liposomes was incubated with 100 μl of styrene beads coated with streptavidin (2 μm in diameter; Polysciences, Warrington, PA) for 2 h at room temperature. The slurry was centrifuged at 5000 × *g* for 5 min, and the beads were resuspended with 4 ml of serum-free DMEM.

Phagocytic Analysis

When indicated, cells (1 × 10^4 cells/coverslip, 22 × 22 mm) were pretreated with 2 μM cytochalasin D (Cyt D), or with the equivalent amount of dimethyl sulfoxide for 30 min at 32 or 37°C in serum-free DMEM. To measure phagocytosis, cells were incubated with 300 μl of bead suspension on each coverslip and incubated at 32 or 37°C for the various time points. Because the kinetics of phagocytosis in Sertoli cell is relatively slow (Filippini *et al.*, 1989), cells were incubated for 6 h to ensure internalization of the beads. Cells were gently washed four times with phosphate-buffered saline (PBS) containing 1.5 mM $CaCl_2$ and 1 mM $MgCl_2$ [PBS (+)]. To distinguish between internalized beads and those attached to the cell surface, the later were labeled with FITC-annexin (BioVision, Mountain View, CA), which specifically binds to PS. For this purpose, cells were incubated with FITC-annexin at room temperature for 10 min. Then, cells were fixed with 2% paraformaldehyde (PFA) in PBS (+). When necessary, cells were permeabilized with 100 μM digitonin to avoid detachment of FITC-annexin from the beads. Mutant cells were determined by immunofluorescence for myc. To quantitate phagocytosis, the annexin-positive and negative beads on the cell surface were counted using phase contrast and fluorescent microscopy. The number of internalized beads was counted in 50 cells randomly chosen from more than 10 independent fields. Phagocytic indices were presented as the number of annexin-negative beads per Sertoli cell. An attachment index was also determined by counting the number of annexin-positive beads per cell.

Microscopy

Sertoli cells (1 × 10^4 cells/coverslip) were fixed with 2% PFA/PBS (+) at room temperature, permeabilized, and subjected to immunocytochemistry (Krauss *et al.*, 2003). The samples were examined using a spinning disk confocal microscope system (CSU10; Yokogawa Electric, Kanazawa, Japan)

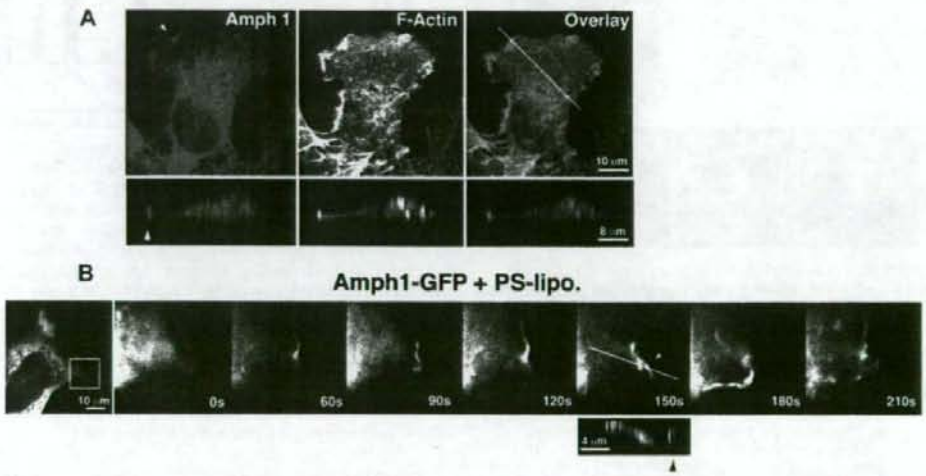

Figure 3. PS-liposomes induce accumulation of amphiphysin 1 at ruffles in Sertoli cells. (A) Ser-W3 cells (1 × 10^4 cells/coverslip) were incubated with 0.25 mM PS liposomes at 37°C for 10 min, and then they were fixed, permeabilized, and stained with anti-amphiphysin 1 antibodies (mab3) (left) and Alexa488-phalloidin (middle). Vertical sections along a line in the overlay image (right) are shown in the bottom panels. The length of the *z*-axis is expanded by four times. Arrowheads indicate the ruffles. Note the colocalization of amphiphysin 1 and F-actin at the ruffles in stimulated cells. (B) Sequential images of Ser-W3 cells expressing amphiphysin 1-GFP under PS liposome stimulation are shown. After Ser-W3 cells were transfected for 24 h with amphiphysin 1-GFP, they were stimulated with PS liposomes, as described in A. Amphiphysin 1 accumulated at the peripheral membrane ruffles that originated at the lamellipodial edge (arrowheads at 150 s). Vertical sections along with lines are shown in the bottom panel. In the vertical sections, the length is expanded by 4 times.

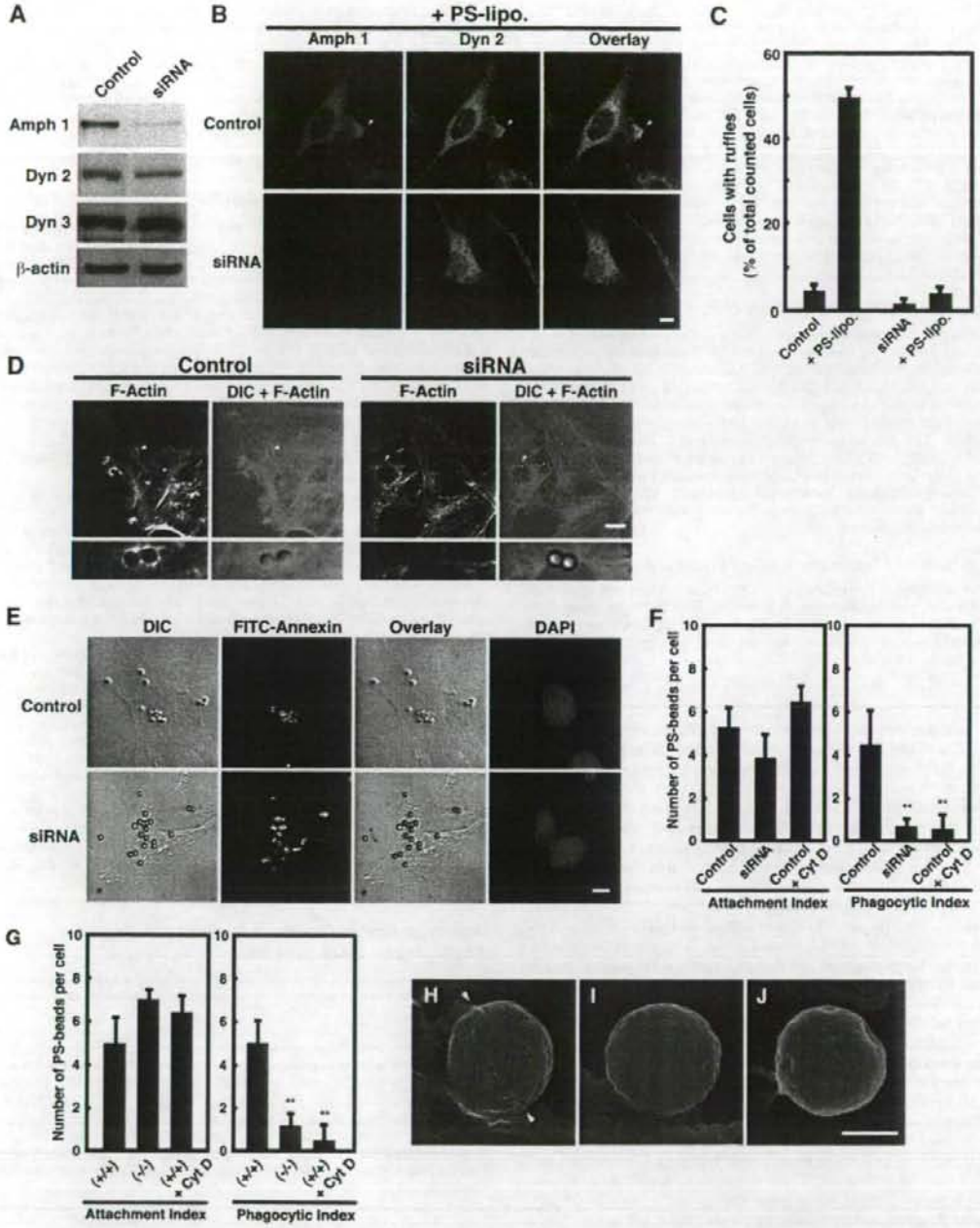

Figure 4. Amphiphysin 1 is required for PS-stimulated membrane ruffling, actin polymerization and phagocytosis. (A) Control siRNA or siRNA for amphiphysin 1 was transfected into Ser-W3 cells. After 48 h, cells were lysed, and 20 μg of lysate was subject to Western blotting by using anti-amphiphysin 1 antibodies (mab3). Dynamin 2, dynamin 3, and β-actin were used as the controls. (B) Control cells and cells treated with amphiphysin 1 siRNA were stimulated with PS liposomes at 0.25 mM at 37°C for 10 min. Cells were labeled with anti-amphiphysin 1 (mab 3) (left) or dynamin 2 (middle) antibodies. The samples were analyzed by fluorescent confocal microscopy. Bar, 10 μm. (C) The number of cells, which were positive for ruffles, was determined and expressed as a percentage of the total number of cells analyzed. One hundred cells in 10 independent fields were counted in each experiment. All results represent the mean ± SEM from the three experiments. (D) Amphiphysin 1 RNAi inhibits actin polymerization during phagocytosis. Control cells or siRNA-treated cells were incubated with PS beads at 37°C for 90 min. Cells were labeled with Alexa488-phalloidin. The samples were analyzed by phase contrast and fluorescent confocal microscopy. PS beads are indicated by arrowheads and are shown at high magnification (bottom). F-actin is observed around the bound beads in control cells (left). The actin polymerization in siRNA-treated cells was barely seen (right). Control cells

combined with an inverted microscope (IX-71; Olympus Optical, Tokyo, Japan) and a CoolSNAP-Pro camera (Roper Industries., Sarasota, FL). The Z-positioning was accomplished by a piezo-electric motor (Olympus Optical) mounted underneath the objective lens. The system was steered by MetaMorph software (Molecular Devices, Sunnyvale, CA). Z-series images were taken at 0.2-μm increments. Vertical images were reconstituted from the Z-series of images by MetaMorph. For live imaging, cells (1×10^4 cells/coverslip) were cultured at 37 or 32°C for 3 d on collagen type I-coated coverslips (12 mm in diameter), and then they were transfected with human amphiphysin 1-GFP at the concentration of 1 μg per coverslip. Live-cell confocal time-lapsed images were taken using a spinning disk confocal microscope system (CSU10) combined with an inverted microscope (IX-71) and a CoolSNAP-Pro camera (Tadakuma *et al.*, 2001). Images were automatically captured every 30 s. Vertical images were reconstituted from a Z-series of images by MetaMorph, as described above. When necessary, images were further processed using Adobe Photoshop and Illustrator software (Adobe Systems, Mountain View, CA).

Small-interfering RNA (siRNA)-mediated Interference

Preannealed siRNA for rat amphiphysin 1, and negative control siRNA were synthesized and purified by Ambion (Austin, TX). The sequences for siRNA are as follows: rat amphiphysin 1, 5′-GGCAGAUGAAACAAAAGAUtt-3′ for oligo 1, 5′-GGUAUGCAGGAGGCCUCAAtt-3′ for oligo 2, and 5′-GGAGAACAUCAUCAAUUUCtt-3′ for oligo 3. Scrambled RNA that has no significant sequence homology to mouse, rat, or human gene sequences was used as the negative control. The day before transfection, cells were plated in six-well plates (5.0×10^4 cells/well). Two hundred picomoles of duplex siRNA was transfected into the cells using 4 μl of Lipofectamine 2000 (Invitrogen). After 48 h, the cells were subjected to the different experiments. We confirmed that all three transfections of siRNA for amphiphysin 1 were effective, and we obtained essentially the same results.

Quantification of Membrane Ruffle Formation

Liposomes were added to Ser-W3 cells (1×10^4 cells/coverslip) at 0.25 mM in serum-free DMEM and incubated at 37°C for 10 min. The cells were then washed with PBS (+) three times. Stimulated or control Sertoli cells were fixed, permeabilized, and stained with anti-amphiphysin 1 antibodies (mab 3; provided by Dr. De Camilli, Yale University) or anti-c-myc antibodies and Alexa488- or rhodamine-phalloidin. Cells with peripheral ruffles were characterized as cells with thick peripheral actin filament accumulation according to Suetsugu *et al.* (2003). When counting the cells with ruffles, cells with free edges were selected. To quantify ruffling efficiency, cells that had no ruffles were scored as negative, whereas cells that had one or more ruffles were considered to be positive. The number of cells that were positive for ruffles was counted and expressed as a percentage of total number of cells analyzed. At least 100 cells in different areas of the wells were counted in each experiment.

Preparation for Testis Cytosol

Testis cytosol was prepared as described previously (Ma *et al.*, 1998b). Briefly, 20 testis of amph 1 (+/+) or amph 1 (−/−) mice were homogenized in 5 ml of XB buffer (10 mM HEPES, 100 mM KCl, 2 mM $MgCl_2$, 0.1 mM $CaCl_2$, 5 mM EGTA, 50 mM sucrose, 1 mM dithiothreitol, 1 μg/ml leupeptin, 5 μg/ml pepstatin, and 0.4 mg/ml phenylmethylsulfonyl fluoride), pH 7.4. The homogenate was centrifuged at $3000 \times g$ for 20 min and $10,000 \times g$ for 20 min. The resultant supernatant was diluted with XB buffer to 4 times in volume and centrifuged at $400,000 \times g$ for 1 h. The clear supernatant was carefully removed and concentrated to 4 times in volume in Centriprep-10 concentrators (Millipore, Billerica, MA). A final concentration of the cytosol was 40–50 mg/ml. Monomer actin in amph 1 (−/−) and amph 1 (+/+) cytosol was determined to be equal as estimated by Western blotting. In recovery experiments, recombinant amphiphysin 1 or mutants were purified as described previously (Yoshida *et al.*, 2004), and added to amph 1 (−/−) cytosol.

In Vitro Actin Assembly Assay

For visual assay for actin assembly, cytosol (20 mg/ml) was incubated at room temperature with liposomes (0.15 mM) and rhodamine-actin (0.4 mg/ml/coverslip; Invitrogen). Samples were supplemented with ATP generating system (1 mM ATP, 8 mM creatine phosphate, and 8 U/ml phosphocreatine kinase), 1.3 mM $MgCl_2$, and 0.1 mM EGTA. The mixture was examined by confocal microscopy. MetaMorph software controlled the microscope functions, and it was used for image processing.

For quantitative analysis of actin assembly, pyrene-actin assay was carried out according to Ma *et al.* (1998b) with slight modification. Ma *et al.* (1998b) first mixed all the components except liposomes and then added the liposomes. The sequence was altered to ensure all the components mixed uniformly in the cuvette. Briefly, 125 μl of XB buffer was incubated in a quartz cuvette at room temperature for 5 min. Then, an ice-cold mixture of liposomes (50 μM) and cytosol (8 or 16 mg/ml) supplemented with 0.4 mg/ml pyrene-actin (Cytoskeleton, Denver, CO), 1.3 mM $MgCl_2$, 0.1 mM EGTA, and ATP generating system (1 mM ATP, 8 mM creatine phosphate, and 8 U/ml phosphocreatine kinase) was added to the buffer. Pyrene fluorescence was measured at 407 nm with excitation at 365 nm in an F-2500 fluorescence spectrophotometer (Hitachi, Tokyo, Japan) with a 10-nm slit width. Fluorescent intensity of the buffer alone was subtracted from that of samples with cytosol and liposomes.

Determination of Residual Bodies in Wild and Amphiphysin 1-deficient Mice

Spermatogenetic stages in mice seminiferous tubules were categorized into XII stages, and the spermatids maturation was classified into 16 steps as described previously (Oakberg, 1956; Abe *et al.*, 1991). To quantify residual bodies in stage VIII, 30 seminiferous tubules each from amph 1 (+/+) or amph 1 (−/−) testis were randomly examined from 5 of amph 1 (+/+) or amph 1 (−/−) mice using hematoxylin and eosin (H&E) staining and light microscopy. Residual bodies and unreleased spermatids were observed in VIII stage, visualized with H&E staining (Beardsley *et al.*, 2003). The size of the residual bodies in stage VIII seminiferous tubules was determined and the average of the areas was calculated. The quantification of the residual body size was determined on light microscopic images of H&E-stained samples. Twenty independent fields were analyzed by Mac Scope software (Mitani, Osaka, Japan).

Scanning Electron Microscopy

Mouse primary-cultured Sertoli cells (1×10^4 cells on coverslip) were incubated with PS coated styrene beads at 32°C for 90 min. After incubation, cells were extensively washed with PBS (+) three times, and one time with 0.1 M cacodylate buffer, pH 7.4. Pairs of coverslips were fixed for 1 h at room temperature with 2% glutaraldehyde in 0.1 M cacodylate buffer, containing 6.8% sucrose (Diakonova *et al.*, 2002). Coverslips were then postfixed with 1% osmium tetroxide in 0.1 M cacodylate buffer for 1 h at 4°C and washed with 0.1 M cacodylate buffer twice. After dehydration with a series of ascending concentrations of ethanol, the coverslips were coated with osmium tetroxide by using an ion coater. Cells were observed with a scanning electron microscope (S900; Hitachi).

Figure 4 (facing page). displayed actin polymerization with ~67.5 ± 10.7% of the associated beads. In contrast, the polymerization occurred with only 10.2 ± 4.0% of associated beads in siRNA-treated cells. (For both treatments, n = 90 cells, from three independent experiments). Bar, 10 μm. (E) Effect of RNAi on amphiphysin 1 in PS-dependent phagocytosis. Control cells and siRNA-treated cells were incubated with PS beads for 6 h at 37°C, and then washed. Control cells were pretreated with Cyt D at 2 μM for 30 min as negative control. Cells were incubated with FITC-annexin at room temperature for 10 min before fixation to determine the level of bead internalization. Bar, 10 μm. (F) Quantitation of levels of phagocytosis in control cells or siRNA-treated cells. Annexin-positive and -negative beads were counted on the cell surface by using phase contrast and fluorescent confocal microscopy. The number of internalized beads was determined in 50 randomly chosen cells from 10 independent fields. Phagocytic index was quantified as the number of annexin-negative beads per cell. The attachment index was determined by counting the number of annexin-positive beads per cell. All results are reported as means ± SEM from three experiments. Statistical significance was determined by Student's *t* tests (**$p < 0.01$). (G) Phagocytic activity in the amph 1 (+/+) or amph 1 (−/−) primary cultured Sertoli cells. Cells were processed for phagocytic activity as described in F. Cells from amph 1 (+/+) were pretreated with Cyt D for 30 min at 32°C as negative control. Results are reported as means ± SEM from three experiments. Statistical significance was determined by Student's *t* tests (**$p < 0.01$). (H–J) We performed scanning electron microscopy to determine PS-dependent phagocytosis in primary cultured mouse Sertoli cells. Sertoli cells from amph 1 (+/+) or amph 1 (−/−) mice were fixed after 90 min of incubation with PS beads and then imaged. Cells from amph 1 (+/+) were pretreated with Cyt D for 30 min at 32°C as negative control. In amph 1 (+/+) Sertoli cells, phagocytic cups were evident (H, arrowheads). In contrast, the amph 1 (−/−) Sertoli cells displayed incomplete membrane extension and demonstrated low abilities to engulf the beads (I). Similarly, phagocytic cup formation was not observed in Cyt D-treated wild-type Sertoli cells (J). In this image, beads were highlighted using Adobe Photoshop CS2. Bar, 1.5 μm.

RESULTS

Amphiphysin 1 Is Involved in PS-dependent Phagocytosis

The last step of germ cell maturation includes the elimination of the spermatid cytoplasm before their release. This occurs at stage VIII of the seminiferous tubules. Sertoli cells use phagocytic mechanisms to internally incorporate the germ cell cytoplasm (Clermont *et al.*, 1987). The incorporated cytoplasm, termed residual bodies, can be seen in the Sertoli cells with hematoxylin and eosin staining (Beardsley and O'Donnell, 2003). We analyzed amph 1 (−/−) Sertoli cells to investigate whether amphiphysin 1 is implicated in the phagocytic process of the residual bodies. In stage VIII of the seminiferous tubules, we saw round eosinophilic residual bodies adjacent to mature spermatids along the luminal surface of the tubule (Figure 1, B and D). The residual bodies were clearly larger in the amph 1 (−/−) testis versus the wild type (Figure 1, B and D). Morphological analysis revealed that the average size of the residual bodies in amph 1 (−/−) is ~1.8 times larger than that of amph 1 (+/+) (Figure 1E), suggesting that residual body uptake or phagosome formation is reduced in the amph 1 (−/−) Sertoli cells.

Phagocytosis of residual bodies is triggered by the recognition of PS moieties on the outer surface of germ cells (Blanco-Rodriguez and Martinez-Garcia, 1999). A similar mechanism is thought to be used when Sertoli cells phagocytose apoptotic germ cells (Shiratsuchi *et al.*, 1997, 1999; Kawasaki *et al.*, 2002). Therefore, we examined the mechanisms of the phagocytic processes in the presence of apoptotic germ cells. Apoptosis of germ cells was induced using camptothecin (Fusaro *et al.*, 2003), and the germ cells were placed on primary cultured rat Sertoli cells. As shown in Figure 1F, amphiphysin 1 and F-actin accumulated at the phagocytic cup formed on the surface of the cells. Consistent with previous report (Kamitani *et al.*, 2002), amphiphsyin 1 was absent in the germ cells. To further elucidate the function of amphiphysin 1 in phagocytosis, we measured the uptake of PS coated styrene beads (PS beads) by primary cultured rat Sertoli cells, or by Sertoli cell lines. We observed an accumulation of endogenous or exogenous amphiphysin 1 and F-actin at the phagosomes in Ser-W3 cells, Sertoli cell line (Figure 2A), and in TM4 cells, mouse Sertoli cell line (Supplemental Figure 1). Ser-W3 cells specifically associated to PS beads, but not to phosphatidylcholine (PC)-coated beads (Figure 2, B and C). The association of the PS beads with the cells was abolished by preincubation of the cells with PS liposomes or with anti-SR-BI antibodies that recognize the ectodomain of the receptor (Gu *et al.*, 2000) (Figure 2, B and C). In this experimental system, we confirmed that phagocytosis is dependent on both PS and the PS receptor SR-BI.

PS-Liposomes Induce Amphiphysin 1-positive Peripheral Ruffles

Phagocytosis requires actin polymerization, which causes dynamic membrane remodeling to form the characteristic membrane ruffling and pseudopods (Caron and Hall, 1998; Anderem and Underhill, 1999). We examined ruffle formation in PS liposome-stimulated Sertoli cells. The ruffles were readily observed as actin-rich protrusions at the cell periphery (Suetsugu *et al.*, 2003). Approximately half of the Ser-W3 cells formed ruffles upon liposomal stimulation (Figures 3 and 4C). Vertical sectioning revealed that both amphiphysin 1 and the actin filaments were colocalized at the tip of leading edge of the ruffles (Figure 3A). In contrast, PC liposomes had no effect on cellular membranes (data not shown). Time-lapsed observations of amphiphysin 1-GFP revealed that amphiphysin 1-positive peripheral ruffles were visible within 60 s after the application of the PS liposomes. These peripheral ruffles occasionally bent up and moved backward as described previously (Figure 3B; Suetsugu *et al.*, 2003).

To test the possibility that amphiphysin 1 might function in ruffle formation, endogenous amphiphysin 1 was knocked down in Ser-W3 cells by RNAi, and the cells were studied for both PS-dependent membrane changes and phagocytosis. The expression of amphiphysin 1 was decreased by ~95% by the RNAi. The expression of dynamin 2 was decreased by ~20%, and expression of dynamin 3 and β-actin was unaffected (Figure 4A). Depletion of amphiphysin 1 in Sertoli cells by RNAi caused smaller cell shape and slight cell detachment. In the siRNA-treated Sertoli cells, both localization of clathrin and transferrin uptake were unchanged, suggesting that depletion of amphiphysin 1 does not affect on clathrin-mediated endocytosis (Supplemental Figure 2). Stimulation of control cells with PS liposomes for 10 min resulted in the formation of apparent ruffles, which accumulated amphiphysin 1 and dynamin 2 (Figure 4B), whereas ruffle formation in the siRNA-treated cells decreased by ~90% of control (Figure 4C). Transfection of amphiphysin 1 cDNA into siRNA-treated cells restored the ruffle formation (Supplemental Figure 3).

We then examined actin polymerization during uptake of the PS beads. In the control cells, PS beads were associated with the membranes, and they were surrounded by F-actin. In contrast, F-actin was present much less around the beads in the siRNA-treated cells (Figure 4D). As expected, PS-dependent phagocytosis in siRNA-treated cells was reduced to 15% of the control (Figure 4, E and F).

The role of amphiphysin 1 in PS-dependent phagocytosis was also confirmed using primary cultured Sertoli cells from amph 1 (−/−) mice. In the amph 1 (−/−) cells, the number of PS beads attached on the cell surface was unchanged compared with that in the wild type, but uptake of the beads was decreased by 80% in amph 1 (−/−) cells (Figure 4G). Electron scanning microscopy revealed that wild-type Sertoli cells engulfed the PS beads through membrane extension (Figure 4H). In contrast, PS beads attached to amph 1 (−/−) Sertoli cells were rarely engulfed by the plasma membrane (Figure 4I). Similarly phagocytic cup formation was not observed in Cyt D-treated wild-type Sertoli cells (Figure 4J). These results indicate that amphiphysin 1 is required for the actin polymerization that causes membrane deformation at the early stage of PS-dependent phagocytosis.

Overexpression of BAR Deletion Mutant Inhibits the Membrane Ruffling and Phagocytosis

We hypothesized that a functional domain of amphiphysin 1 is required for the ruffle formation and phagocytosis. To test this, we used amphiphysin deletion mutants shown in Figure 5A. Wild-type and ΔCLAP amphiphysin 1 transiently expressed in Ser-W3 cells were present as punctate pattern by immunofluorescence, whereas ΔBAR and ΔSH3 were diffusely distributed throughout the cytoplasm (Figure 5B). The expression of ΔBAR in the cells strongly inhibited both PS-dependent ruffle formation and phagocytosis (Figure 5, C and D). ΔBAR-expressing cells were unable to form extensions and tended to be smaller than cells expressing the other mutants (Figure 5B). Expression of ΔSH3 inhibited ruffle formation by ~35% compared with that of control, but the mutant proteins still localized to the ruffles (Figure 5B). Expression of ΔCLAP did not affect ruffle formation but phagocytosis was inhibited by ~30% (Figure 5, C and D).

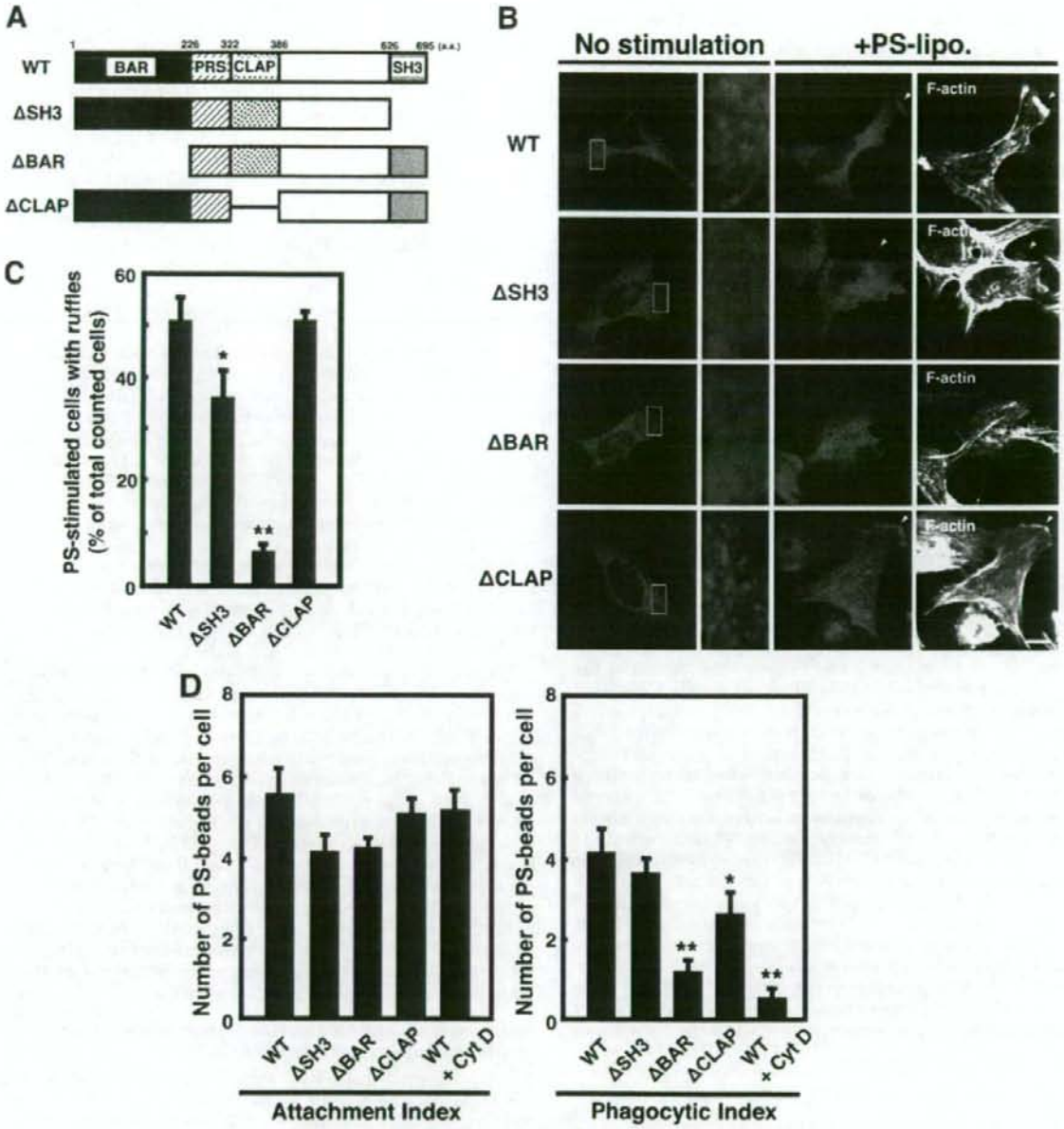

Figure 5. BAR domain of amphiphysin 1 is required for PS-dependent ruffle formation and phagocytosis. (A) Shown are the domain structures of the amphiphysin 1 constructs used in these assays. The numbers indicate the amino acid residues of full-length amphiphysin 1. (B) Effect of the truncated mutants of amphiphysin 1 on PS-dependent ruffle formation. Ser-W3 cells transiently expressing amphiphysin 1-myc, ΔSH3-myc, ΔBAR-myc, or ΔCLAP-myc were stimulated with 0.25 mM of PS liposomes for 10 min at 37°C. The stimulated or untreated cells were then fixed, permeabilized, and labeled with rabbit anti-myc antibodies to detect the expression of wild type (WT) and mutants. Area enclosed with rectangles in the untreated cells is shown at high magnification. F-actin was visualized by Alexa488-phalloidin. Bar, 10 μm. (C) The efficiency of ruffle formation was determined on 50 transfected cells from 10 independent fields as described in Figure 4C. The mean ± SEM of the three independent experiments is plotted. Statistical significance was determined by Student's *t* tests (*$p < 0.05$, **$p < 0.01$). (D) Effect of the truncation mutant of amphiphysin 1 on PS-dependent phagocytosis. Ser-W3 cells transiently expressing the wild type, ΔSH3, ΔBAR, or ΔCLAP mutants were allowed to phagocytose PS beads for 6 h at 37°C. The number of internalized beads was counted in 50 transfected cells randomly chosen from 10 independent fields. The attachment index, defined as beads bound per cell and phagocytic index, defined as beads internalized per cell, was determined as described in Figure 4E. The mean ± SEM of the three independent experiments is plotted. Statistical significance was determined by Student's *t* tests (*$p < 0.05$, **$p < 0.01$).

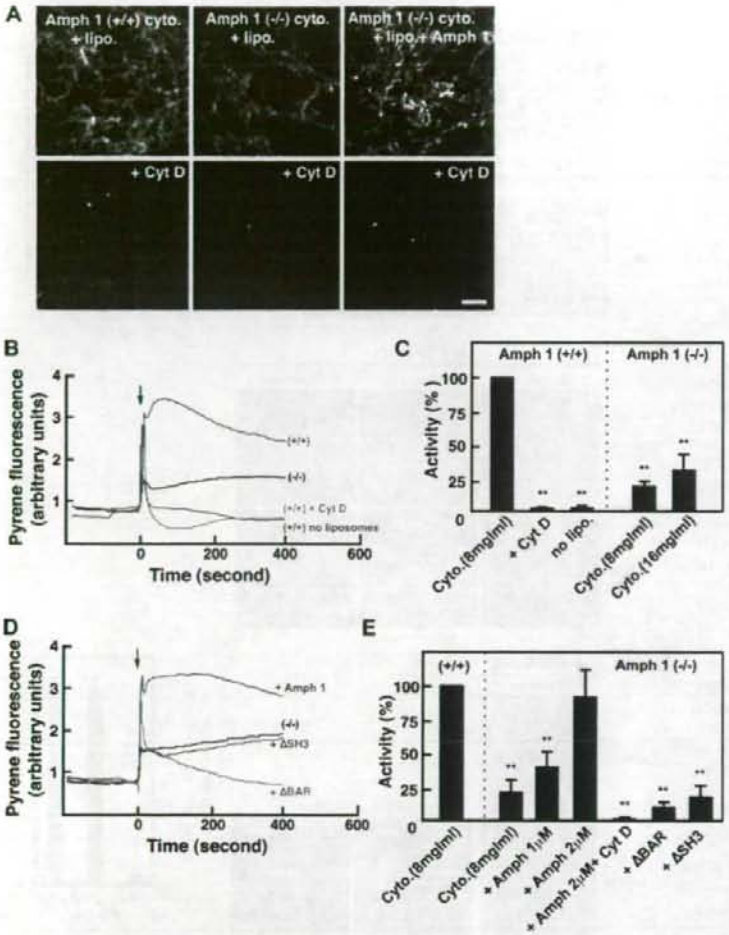

Figure 6. $PI(4,5)P_2$ induced actin polymerization is reduced with amph (−/−) testis cytosol. (A) Actin polymerization was monitored by a visual assay in which 1 μM rhodamine-actin was used to follow actin polymerization by fluorescent confocal microscopy. The cytosol of amph 1 (+/+) and amph 1 (−/−) testis at a concentration of 20 mg/ml was prepared. Control cytosol (top) or cytosol pretreated with 10 μM (Cyt D) for 5 min (bottom) were mixed with liposomes composed of 30% PS, 46% PC, 20% cholesterol, and 4% $PI(4,5)P_2$. To determine the recovery of activity, 2 μM recombinant amphiphysin 1 was added to the cytosol before mixing. After 15 min of incubation at room temperature, the mixtures were analyzed by fluorescent confocal microscopy. Bar, 10 μm. (B) The liposomes-induced actin polymerization was measured using pyrene fluorescence. Cytosol from amph 1 (+/+) testis (red line) or amph 1 (−/−) testis (black line) were treated with 50 μM PS/PC/Chol liposomes containing 4% of $PI(4,5)P_2$. As controls, the incubation was carried out in presence of 10 μM Cyt D (green line), or in absence of liposomes (blue line). The arrow indicates the time when the liposomes and cytosol were added. (C) Comparison of the actin polymerization activity between amph 1 (+/+) and amph 1 (−/−) cytosol is shown. To avoid effect of the initial peak, activity of F-actin formation at 100 s was measured by pyrene-actin fluorescent intensity. All activities are normalized to that of the amph 1 (+/+) testis cytosol. The mean ± SEM of three independent experiments is plotted. Note the reduced actin polymerization in amph 1 (−/−) cytosol compared with the polymerization in the amph 1 (+/+) cytosol. Statistically significant differences from the value of Amph (+/+) cytosol are indicated by (**$p < 0.01$) (Student's *t* test). (D) The liposomes-induced actin polymerization measured by pyrene fluorescence demonstrated the recovery of F-actin formation by recombinant amphiphysin. Amph 1 (−/−) cytosol (black line) was supplemented with 2 μM recombinant full-length amphiphysin 1 (red line), with ΔSH3 mutant (blue line) or with ΔBAR mutant (green line). The incubation and the measurement of activity were carried out as described in B. The arrow indicates the time when the lipids and the cytosol were added. (E) F-actin formation after 100 s induction in amph 1 (−/−) cytosol treated with liposomes containing $PI(4,5)P_2$ alone, with recombinant full-length amphiphysin 1, with ΔSH3 mutant or with ΔBAR mutant was measured by pyrene-actin fluorescence. The recombinant mutant proteins in the mixture were at a concentration of 2 μM. The incubation with 2 μM recombinant full-length amphiphysin 1 was carried out in presence of 10 μM Cyt D as a control. All activities are normalized to that in amph (+/+) cytosol. The mean ± SEM of three independent experiments is plotted. Statistically significant differences from the value of amph (+/+) cytosol are indicated by (**$p < 0.01$) (Student's *t* test).

These results suggest that the BAR domain of amphiphysin 1 is essential for ruffle formation and phagocytosis, whereas the SH3 domain and the CLAP domain may have regulatory functions at different steps of PS-dependent phagocytosis.

Actin Polymerization Induced by Liposomes Is Decreased in Amph 1 (−/−) Cytosol

Because amphiphysin 1 RNAi and the expression of the amphiphysin mutants partly inhibited ruffle formation and phagocytosis, we examined the effect of amphiphysin 1 on $PI(4,5)P_2$-dependent actin polymerization using testis cytosol prepared from amph 1 (+/+) or amph 1 (−/−) mice. Actin polymerization in the cytosol can be induced by incubation of the cytosol with liposomes containing $PI(4,5)P_2$ or phosphatidylinositol-3,4,5-trisphosphate (Ma *et al.*, 1998ab).

Actin polymerization of amph 1 (+/+) and amph 1 (−/−) cytosol was visualized by using rhodamine-actin. When liposomes containing $PI(4,5)P_2$ were added to amph 1 (+/+) cytosol, F-actin started to appear as bright spots within 5 min, and massive actin bundles were visible after 15 min (Figure 6A). The polymerization was abolished by pretreatment of the cytosol with Cyt D or by absence of the liposomes (Figure 6A; data not shown). Not surprisingly, there was less actin polymerization in the amph 1 (−/−) cytosol (Figure 6A). Supplementation of the amph 1 (−/−) cytosol with recombinant amphiphysin 1 recovered actin polymerization to levels comparable with the amph 1 (+/+) cytosol (Figure 6A).

To determine the actin assembly in a quantitative manner, we monitored the activity with pyrene-conjugated actin and polymerization-derived fluorescence. Consistent with the

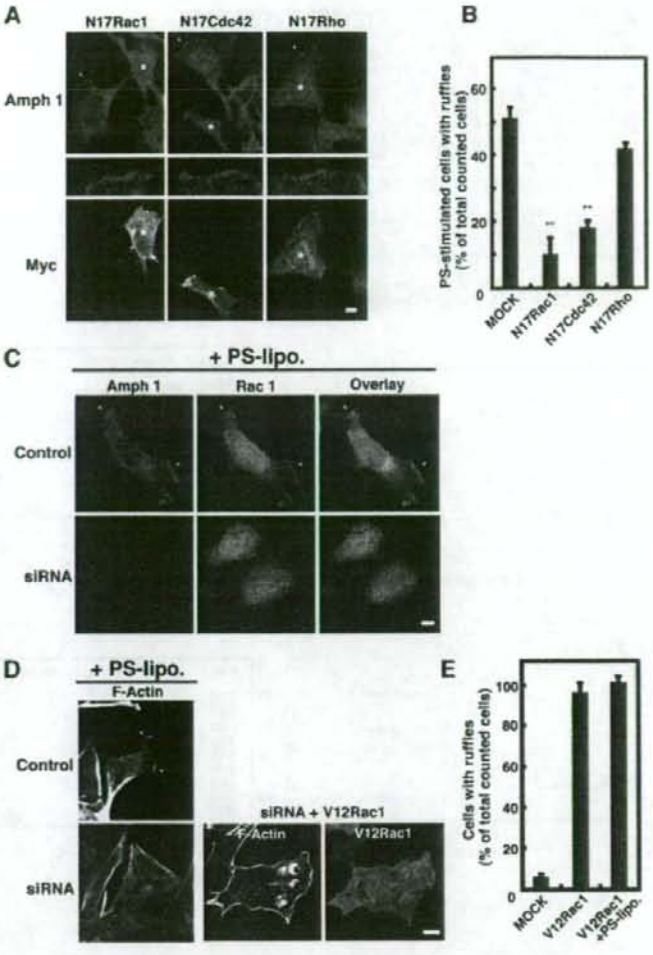

Figure 7. Rac1 is involved in amphiphysin 1-positive ruffle formation. (A) Effect of dominant-negative mutant of Rac1 or Cdc42 on amphiphysin 1-positive ruffle formation. Ser-W3 cells were transfected with myc-N17Rac, -N17Cdc42, or -N17Rho. After 24 h of transfection, cells were stimulated with 0.25 mM of PS liposomes for 10 min, fixed, permeabilized, and stained with rabbit anti-myc antibodies, anti-amphiphysin 1 antibodies (mab 3). Asterisks show where there was expression of mutant Rho GTPases. The ruffles indicated by arrowheads are enlarged on the middle panels. Note that the expression of N17Rac1 strongly inhibited PS-stimulated membrane ruffling (left). Transfection of N17Cdc42 also caused inhibition on ruffle formation in response to PS-stimulation (middle). N17Rho-transfected cells showed a slight inhibition of membrane ruffling (right). Bar, 10 μm. (B) The number of ruffle-positive cells that expressed mutant small G proteins was counted as described in Figure 4C. Fifty cells expressing each small G protein mutant were analyzed in 10 independent fields. All results represent the mean ± SEM from three experiments. Statistically significant differences are indicated by (**$p < 0.01$) (Student's t test). (C) RNAi for amphiphysin 1 impaired the recruitment of endogenous Rac1 to the plasma membrane in Ser-W3 cells. SiRNA-treated (bottom) or control Ser-W3 (top) cells were incubated with 0.25 mM PS liposomes at 37°C for 10 min. The cells were stained with both mouse-anti-amphiphysin 1 antibodies (mab 3) (left) and rabbit-anti-Rac1 antibodies (middle). Bar, 10 μm. (D) Constitutively active Rac1 rescued ruffle formation in amphiphysin 1 siRNA-treated Ser-W3 cells. After 48-h transfection with siRNA for amphiphysin 1 or control siRNA, myc-V12Rac1 (middle) or vector only (left) was later transfected into the cells. Cells were stimulated as described in Figure 7A and stained with rabbit-anti-myc antibodies (right) and rhodamine-phalloidin (middle). Bar, 10 μm. (E) The number of ruffle-positive cells expressing myc-V12Rac1 proteins, with or without PS-stimulation, was counted as described in Figure 4C. Fifty cells expressing each small G protein mutant were analyzed in 10 independent fields. All results represent the mean ± SEM from three experiments.

visual polymerization assay described above, rapid actin assembly was induced by the liposomes in amph 1 (+/+) cytosol (Figure 6, B and C). The polymerization did not occur in the absence of the liposomes or with pretreatment of the cytosol with Cyt D (Figure 6, B and C). Under the same conditions, the actin polymerization in the amph 1 (−/−) cytosol was ~25% of that in amph 1 (+/+) cytosol (Figure 6, B and C). The addition of recombinant amphiphysin 1 to amph 1 (−/−) cytosol was sufficient to recover polymerization activity (Figure 6, D and E). However, the addition of ΔSH3 and ΔBAR proteins could not recover the actin polymerization in amph 1 (−/−) cytosol (Figure 6, D and E). These results suggested that amphiphysin 1 regulates actin polymerization and that the regulation requires for both BAR and SH3. Addition of ΔBAR protein to amph 1 (−/−) cytosol even decreased F-actin formation, suggesting the mutant might depolymerize or destabilize F-actin (Figure 6, D and E).

Pathway of Amphiphysin-positive Ruffle Formation May Be Involved in Rac

It is well known that actin polymerization and ruffle formation are stimulated by the activation of the Rho GTPase family (Ridley, 2001; Cox and Greenberg, 2001). We hypothesized that amphiphysin 1 may be involved in the process of Rho GTPase family-dependent ruffle formation. As shown in Figure 7A and B, expression of dominant-negative Rac1 or Cdc42 (N17Rac1 or N17Cdc42) blocked PS-induced ruffle formation by 85 and 65%, respectively. Dominant-negative Rho slightly inhibited PS-dependent ruffle formation. Furthermore, endogenous Rac 1 and amphiphysin 1 colocalized to the ruffles in the PS-stimulated Ser-W3 cells (Figure 7C). Amphiphysin 1 siRNA treatment inhibited both the recruitment of Rac1 to the membrane and ruffle formation in the PS-stimulated cells (Figure 7C). The overexpression of V12Rac1, a constitutively active mutant of Rac1, in the siRNA-treated cells caused the recovery of ruffle formation (Figure 7, D and E). These results strongly suggest that amphiphysin 1 is involved in Rac1-dependent actin polymerization and that it may function upstream of this protein.

DISCUSSION

In this study, we investigated the role of amphiphysin 1 in Sertoli cell phagocytosis by using knockout animals and cell

culture. We demonstrated that amphiphysin 1 is required for PS-dependent phagocytosis in Sertoli cells and that the protein is crucial for actin polymerization during the process. To our knowledge, this is the first indication that amphiphysin 1 regulates actin dynamics.

Amphiphysin 1 Is Involved in PS-dependent Phagocytosis in Sertoli Cells

Phagocytosis in Sertoli cells contributes to removal of the residual bodies, which occur just before sperm release (Clermont *et al.*, 1987). In amph 1 (−/−) testis, the residual bodies were prominent, suggesting that the phagocytic process is decreased. Consistent with this finding, the numbers of unreleased spermatids were increased in amph 1 (−/−) testis (our unpublished data).

On PS-stimulation of cultured Sertoli cells, amphiphysin 1 accumulated at F-actin–rich structures such as phagocytic cups, phagosomes, or ruffles. Formation of these structures was abolished by amphiphysin 1 RNAi, causing a decrease in phagocytic activity. These results clearly show that amphiphysin 1 is essential for phagocytosis and suggest a role of the molecule in actin dynamics. Although amphiphysin 1 functions in clathrin-mediated endocytosis in the neuronal synapse (Takei *et al.*, 1999), both transferrin uptake and clathrin localization in Sertoli cells were unchanged by RNAi (Supplemental Figure 2), indicating that the main cellular function of amphiphysin 1 in the Sertoli cells is phagocytosis.

We demonstrated that the BAR domain of amphiphysin 1 is required for both PS-dependent ruffle formation and for phagocytosis. It has been reported that BAR domain is responsible for homo- or heterodimerization of amphiphysins (Wigge *et al.*, 1997; Friesen *et al.*, 2006), sensing membrane curvature, (Peter *et al.*, 2004; Yoshida *et al.*, 2004), and membrane deformation (Takei *et al.*, 1999). These characteristics of BAR domain might be required for ruffle formation and phagocytosis.

It is possible that inhibition of ruffle formation by ΔBAR mutant is indirect. Because ΔSH3 mutant, which contains BAR domain partially inhibited the ruffle formation, suggesting that binding molecules via SH3 domain may be involved. In addition, because ΔSH3 mutant still localized at ruffles, the mutant may form partially functional dimer with endogenous amphiphysin 1. ΔBAR mutant contains proline-rich stretch (PRS), CLAP and SH3, which can bind to functional proteins required for ruffle formation. In particular, the SH3 domain of amphiphysin 1 interacts with dynamin 2, which has been suggested to be involved in formation of membrane ruffling (McNiven *et al.*, 2000; Schafer, 2004). In this study, expression of dynamin 2 was decreased by 20% in amphiphysin 1 knocked down cells. Because amphiphysin 1 binds to dynamin 2, some of free dynamin 2 may be degraded in the absence of amphiphysin 1. It is unlikely, however, that the decrease of dynamin 2 contributes to the inhibition of ruffle formation. Because exogenous amphiphysin 1 rescued ruffle formation in amphiphysin 1 depleted Sertoli cells. Furthermore, clathrin-mediated endocytosis was not changed in siRNA-treated cells, suggesting that dynamin 2 is still functional in the cell (Supplemental Figure 3).

ΔCLAP inhibited by ~30% of PS-dependent phagocytosis. It has been reported that clathrin accumulates at nascent phagosomes to assist in the recycle of membranes and receptors (Aggeler and Werb, 1982), and the CLAP domain may contribute to this process. Amphiphysin 2m, an isoform lacking a CLAP domain, has known functions in phagocytosis in macrophages (Gold *et al.*, 2000), suggesting the presence of different phagocytic pathway in this cell type.

Amphiphysin 1 Regulates Actin Polymerization

Phagocytosis involves actin dynamics regulated by the Rho GTPase family (Cox *et al.*, 1997; Tolias *et al.*, 2000; Bokoch, 2005). In the ruffling area, an increased production of $PI(4,5)P_2$ activates the Rho GTPase family proteins, such as Cdc42 or Rac (Czech, 2000). These in turn stimulate actin polymerization by the Arp 2/3 complex and the WASP family (Chimini and Chavrier, 2000). As shown in Figure 6, $PI(4,5)P_2$-induced F-actin formation was significantly reduced in the amph 1 (−/−) cytosol. This effect was restored by the addition of recombinant full-length amphiphysin 1, but not by ΔBAR or ΔSH3, suggesting that BAR and SH3 domain are necessary for recruitment of amphiphysin 1 to membrane, and for recruitment of its binding proteins required for F-actin formation, respectively.

It has been reported that dynamin 2 is involved in actin dynamics as well as ruffle formation (Kruchten and McNiven, 2006). Dynamin 2 binds to cortactin, which specifically binds to F-actin (McNiven *et al.*, 2000; Schafer, 2004). Furthermore, dynamin 2 interacts with Rac1 and has been implicated both in the formation of ruffles (Krueger *et al.*, 2003) and in the regulation of the localization of intracellular Rac1 (Schlunck *et al.*, 2004). In addition, *Drosophila* amphiphysin interacts with neural Wiskott-Aldrich syndrome protein, and this interaction is necessary for the morphogenesis of rhabdomere microvilli (Zelhof and Hardy, 2004). Thus, amphiphysin 1 may indirectly function on actin dynamics.

The dominant-negative mutant of Rac1 or Cdc42 abolished the formation of amphiphysin 1-positive ruffles. In addition, amphiphysin 1 RNAi inhibited ruffle formation, but constitutively active Rac1 expression in the siRNA-treated cells rescued it, indicating that amphiphysin 1 functions upstream of Rac1. Consistently, amphiphysin 1 is known to bind to the proline-rich domains of RICH-1, a RhoGAP protein (Richnau *et al.*, 2004). Additionally, direct binding of the yeast amphiphysin homologue RVS to actin has been shown in a yeast two-hybrid system (Amberg *et al.*, 1995).

In conclusion, we have demonstrated that amphiphysin 1 participates in phagocytosis by changing actin polymerization activity in Sertoli cells. Amphiphysin 1 is implicated in the signaling pathway that involves Rac1 and Cdc42. The precise role of amphiphysin 1 in the actin–regulatory signal cascade should to be elucidated with further studies.

ACKNOWLEDGMENTS

We thank Pietro De Camilli (Yale University) for providing amphiphysin 1 knockout mice and Toshiki Ito (Kobe University) for providing the plasmids pEF-BOS-myc-N17Rac1, V12Rac1, N17Cdc42, and N17Rho. This work was supported in part by grants from the Ministry of Education, Science, Sports, and Culture of Japan, the Nissan Science Foundation, the Asahi Glass Foundation, and the Wesco Scientific Promotion Foundation.

REFERENCES

Abe, K., Shen, L. S., and Takano, H. (1991). The cycle of the seminiferous epithelium and stages in spermatogenesis in dd-mice. Hokkaido Igaku Zasshi *66*, 286–299.

Aggeler, J., and Werb, Z. (1982). Initial events during phagocytosis by macrophages viewed from outside and inside the cell: membrane-particle interactions and clathrin. J. Cell Biol. *94*, 613–623.

Amberg, D. C., Basart, E., and Botstein, D. (1995). Defining protein interactions with yeast actin in vivo. Nat. Struct. Biol. *2*, 28–35.

Anderem, A., and Underhill, D. M. (1999). Mechanisms of phagocytosis in macrophages. Annu. Rev. Immunol. *17*, 593–623.

Bauerfeind, R., Takei, K., and DeCamilli, P. (1997). Amphiphysin I is associated with coated endocytic intermediates and undergoes stimulation-dependent dephosphorylation in nerve terminals. J. Biol. Chem. 272, 30984–30992.

Beardsley, A., and O'Donnell, L. (2003). Characterization of normal spermiation and spermiation failure induced by hormone suppression in adult rats. Biol. Reprod. *68*, 1299–1307.

Blanco-Rodriguez, J., and Martinez-Garcia, C. (1999). Apoptosis is physiologically restricted to a specialized cytoplasmic compartment in rat spermatids. Biol. Reprod. *61*, 1541–1547.

Bokoch, G. M. (2005). Regulation of innate immunity by Rho GTPases. Trends. Cell Biol. *15*, 163–171.

Caron, E., and Hall, A. (1998). Identification of two distinct mechanisms of phagocytosis controlled by different Rho GTPases. Science *282*, 1717–1721.

Chemes, H. (1986). The phagocytic function of Sertoli cells: a morphological, biochemical, and endocrinological study of lysosomes and acid phosphatase localization in the rat testis. Endocrinology *119*, 1673–1681.

Chimini, G., and Chavrier, P. (2000). Function of Rho family proteins in actin dynamics during phagocytosis and engulfment. Nat. Cell Biol. 2, E191–E196.

Clermont, Y., Morales, C., and Hermo, L. (1987). Endocytic activities of Sertoli cells in the rat. Ann. N Y Acad. Sci. *513*, 1–15.

Cox, D., Chang, P., Zhang, Q., Reddy, P. G., Bokoch, G. M., and Greenberg, S. (1997). Requirements for both Rac1 and Cdc42 in membrane ruffling and phagocytosis in leukocytes. J. Exp. Med. *186*, 1487–1494.

Cox, D., and Greenberg, S. (2001). Phagocytic signaling strategies: Fc (gamma) receptor-mediated phagocytosis as a model system. Semin. Immunol. *13*, 339–345.

Czech, M. P. (2000). PIP_2 and PIP_3: complex roles at the cell surface. Cell *100*, 603–606.

David, C., McPherson, P. S., Mundigl, O., and DeCamilli, P. (1996). A role of amphiphysin in synaptic vesicle endocytosis suggested by its binding to dynamin in nerve terminals. Proc. Natl. Acad. Sci. USA *93*, 331–335.

Dawson, J. C., Legg, J. A., and Machesky, L. M. (2006). Bar domain proteins: a role in tubulation, scission and actin assembly in clathrin-mediated endocytosis. Trends Cell Biol. *16*, 493–498.

Diakonova, M., Bokoch, G., and Swanson, J. A. (2002). Dynamics of cytoskeletal proteins during Fcgamma receptor-mediated phagocytosis in macrophages. Mol. Biol. Cell *13*, 402–411.

Di Paolo, G. *et al.* (2002). Decreased synaptic vesicle recycling efficiency and cognitive deficits in amphiphysin 1 knockout mice. Neuron *33*, 789–804.

Filippini, A., Russo, M. A., Palombi, F., Bertalot, G., De Cesaris, P., Stefanini, M., and Ziparo, E. (1989). Modulation of phagocytic activity in cultured Sertoli cells. Gamate Res. 23, 367–375.

Friesen, H., Humphrries, C., Ho, Y., Schub, O., Colwill, K., and Andrews, B. (2006). Characterization of the yeast amphiphysin Rvs161p and Rvs167p reveals roles for the Rvs heterodimer in vivo. Mol. Biol. Cell *17*, 1306–1321.

Fusaro, G., Dasgupta, P., Rastogi, S., Joshi, B., and Chellappan, S. (2003). Prohibitin induces the transcriptional activity of p53 and is exported from the nucleus upon apoptotic signaling. J. Biol. Chem. *278*, 47853–47861.

Gillot, I., Jehl-Pietri, C., Gounon, P., Luquet, S., Rassoulzadegan, M., Grimaldi, P., and Vidal, F. (2005). Germ cells and fatty acids induce translocation of CD36 scavenger receptor to the plasma membrane of Sertoli cells. J. Cell Sci. *118*, 3027–3035.

Gold, E. S., Morrissette, N. S., Underhill, D. M., Guo, J., Bassetti, M., and Anderem, A. (2000). Amphiphysin IIm, a novel amphiphysin II isoform, is required for macrophage phagocytosis. Immunity *12*, 285–292.

Greenberg, S., and Grinstein, S. (2002). Phagocytosis and innate immunity. Curr. Opin. Immunol. *14*, 136–145.

Gu, X., Kozarsky, K., and Krieger, M. (2000). Scavenger receptor class B, type I-mediated [^{3}H]cholesterol efflux to high and low density lipoproteins is dependent on lipoprotein binding to the receptor. J. Biol. Chem. *275*, 29993–30001.

Kaksonen, M., Toret, C. P., and Drubin, D. G. (2005). A modular design for the clathrin- and actin-mediated endocytosis machinery. Cell *123*, 305–320.

Kamitani, A., Yamada, H., Kinuta, M., Watanabe, M., Li, S. A., Matsukawa, T., McNiven, M. A., Kumon, H., and Takei, K. (2002). Distribution of dynamins in testis and their possible relation to spermatogenesis. Biochem. Biophys. Res. Commun. *294*, 261–267.

Kawasaki, Y., Nakagawa, A., Nagaosa, K., Shiratsuchi, A., and Nakanishi, Y. (2002). Phosphatidylserine binding of class B scavenger receptor type I, a phagocytosis receptor of testicular Sertoli cells. J. Biol. Chem. *277*, 27559–27566.

Krauss, M., Kinuta, M., Wenk, M. R., DeCamilli, P., Takei, K., and Haucke, V. (2003). ARF6 stimulates clathrin/AP-2 recruitment to synaptic membranes by activating phosphatidylinositol phosphate kinase type Iγ. J. Cell Biol. *162*, 113–124.

Kruchten, A. E., and McNiven, M. A. (2006). Dynamin as a mover and pincher during cell migration and invasion. J. Cell Sci. *119*, 1683–1690.

Krueger, E. W., Orth, J. D., Cao, H., and McNiven, M. A. (2003). A dynamin-cortactin-Arp2/3 complex mediates actin reorganization in growth factor-stimulated cells. Mol. Biol. Cell *14*, 1085–1096.

Ma, L. E., Rohatgi, R., and Kirschner, M. W. (1998a). The Arp2/3 complex mediates actin polymerization induced by the small GTP-binding protein Cdc42. Proc. Natl. Acad. Sci. USA *95*, 15362–15367.

Ma, L. E., Cantley, L. C., Janmey, P. A., and Kirschner, M. W. (1998b). Corequirement of specific phosphoinositides and small GTP-binding protein Cdc42 in inducing actin assembly in *Xenopus* egg extracts. J. Cell Biol. *140*, 1125–1136.

McNiven, M. A., Kim, L., Krueger, E. W., Orth, J. D., Cao, H., and Wong, T. W. (2000). Regulated interactions between dynamin and the actin-binding protein cortactin modulate cell shape. J. Cell Biol. *151*, 187–198.

Morales, C. R., and Clermont, Y. (1991). Phagocytosis and endocytosis in Sertoli cells of the rat. Bull. Assoc. Anat. *75*, 157–162.

Mundigl, O., Ochoa, G. C., David, C., Slepnev, V. I., Kabanov, A., and DeCamilli, P. (1998). Amphiphysin I antisense oligonucleotides inhibit neurite outgrowth in cultured hippocampal neurons. J. Neurosci. *18*, 93–103.

Munn, A. L., Stevenson, B. J., Geli, M. I., and Riezman, H. (1995). end5, end6, and end 7, mutations that cause actin delocalization and block the internalization step of endocytosis in *Saccharomyces cerevisiae*. Mol. Biol. Cell 6, 1721–1742.

Niedergang, F., and Chavrier, P. (2004). Signaling and membrane dynamics during phagocytosis: many roads lead to the phagos(R)ome. Curr. Opin. Cell Biol. *16*, 422–428.

Oakberg, E. F. (1956). A description of spermiogenesis in the mouse and its use in analysis of the cycle of the seminiferous epithelium and germ cell renewal. Am. J. Anat. *99*, 391–413.

Peter, B. J., Kent, H. M., Mills, I. G., Vallis, Y., Butler, P. J., Evans, P. R., and McMahon, H. T. (2004). BAR domains as sensors of membrane curvature: the amphiphysin BAR structure. Science *303*, 495–499.

Prognan, F., Masson, M. T., Lagelle, F., and Charuel, C. (1997). Establishment of a rat Sertoli cell line that displays the morphological and some of the functional characteristics of the native cell. Cell Biol. Toxicol. *13*, 453–463.

Richnau, N., Fransson, A., Farsad, K., and Aspenstrom, P. (2004). RICH-1 has a BIN/Amphiphysin/Rvsp domain responsible for binding to membrane lipids and tubulation of liposomes. Biochem. Biophys. Res. Commun. *320*, 1034–1042.

Ridley, A. J. (2001). Rho family proteins: coordinating cell responses. Trends Cell Biol. *11*, 471–477.

Russell, L. D., Ren, H. P., Sinha Hikim, I., Schulze, W., and Sinha Hikim, A. P. (1990). A comparative study in twelve mammalian species of volume densities, volumes, and numerical densities of selected testis components, emphasizing those related to the Sertoli cell. Am. J. Anat. *188*, 21–30.

Schafer, D. A. (2004). Regulating actin dynamics at membranes: a focus on dynamin. Traffic *5*, 463–469.

Schlunck, G., Damke, H., Kiosses, W. B., Rusk, N., Symons, M. H., Waterman-Storer, C. M., Schmidt, S. L., and Schwartz, M. A. (2004). Modulation of Rac localization and function by dynamin. Mol. Biol. Cell *15*, 256–267.

Schmid, S. L., McNiven, M. A., and DeCamilli, P. (1998). Dynamin and its partners: a progress report. Curr. Opin. Cell Biol. *10*, 504–512.

Sivadon, P., Bauer, F., Aigle, M., and Crouzet, M. (1995). Actin cytoskeleton and budding pattern are altered in the yeast rvs161 mutant: the Rvs161 protein shares common domains with the brain protein amphiphysin. Mol. Gen. Genet. *246*, 485–495.

Shiratsuchi, A., Umeda, M., Ohba, Y., and Nakanishi, Y. (1997). Recognition of phosphatidylserine on the surface of apoptotic spermatogenic cells and subsequent phagocytosis by Sertoli cells of the rat. J. Biol. Chem. *272*, 2354–2358.

Shiratsuchi, A., Kawasaki, Y., Ikemoto, M., Arai, H., and Nakanishi, Y. (1999). Role of class B scavenger receptor type I in phagocytosis of apoptotic rat spermatogenic cells by Sertoli cells. J. Biol. Chem. *274*, 5901–5908.

Slepnev, V. I., Ochoa, G. C., Butler, M. H., and DeCamilli, P. (2000). Tandem arrangement of the clathrin and AP-2 binding domains in amphiphysin 1 and

disruption of clathrin coat function by amphiphysin fragments comprising these sites. J. Biol. Chem. *275*, 17583–17589.

Small, J. V., Stradal, T., Vignal, E., and Rotter, K. (2002). The lamellipodium: where motility begins. Trends Cell Biol. *12*, 112–120.

Smythe, E., and Ayscough, K. R. (2006). Actin regulation in endocytosis. J. Cell Sci. *119*, 4589–4598.

Suetsugu, S., Yamazaki, D., Kurisu, S., and Takenawa, T. (2003). Differential roles of WAVE1 and WAVE2 in dorsal and peripheral ruffle formation for fibroblast cell migration. Dev. Cell *5*, 595–609.

Tadakuma, H., Yamaguchi, J., Ishihama, Y., and Funatsu, T. (2001). Imaging of single fluorescent molecules using video-rate confocal microscopy. Biochem. Biophys. Res. Commun. *287*, 323–327.

Takei, K., Slepnev, V. I., Haucke, V., and DeCamilli, P. (1999). Functional partnership between amphiphysin and dynamin in clathrin-mediated endocytosis. Nat. Cell Biol. *1*, 33–39.

Tolias, K. F., Hartwig, J. H., Ishihara, H., Shibasaki, Y., Cantley, L. C., and Carpenter, C. L. (2000). Type Ialpha phosphatidylinositol-4-phosphate 5-kinase mediates Rac-dependent actin assembly. Curr. Biol. *10*, 153–156.

Tran, D., Picard, J. Y., Campargue, J., and Josso, N. (1987). Immunocytochemical detection of anti-Mullerian hormone in Sertoli cells of various mammalian species including human. J. Histochem. Cytochem. *35*, 733–743.

Watanabe, M., Tsutsui, K., Hosoya, O., Tsutsui, K., Kumon, H., and Tokunaga, A. (2001). Expression of amphiphysin I in Sertoli cells and its implication in spermatogenesis. Biochem. Biophys. Res. Commun. *287*, 739–745.

Wigge, P., Kohler, K., Vallis, Y., Doyle, C. A., Owen, D., Hunt, S. P., and McMahon, H. T. (1997). Amphiphysin heterodimers: potential role in clathrin-mediated endocytosis. Mol. Biol. Cell *8*, 2003–2015.

Wigge, P., and McMahon, H. T. (1998). The amphiphysin family of proteins and their role in endocytosis at the synapse. Trends Neurosci. *21*, 339–344.

Yoo, J., Jeong, M. J., Kwon, B. M., Hur, M. W., Park, Y. M., and Han, M. Y. (2002). Activation of dynamin I gene expression by Sp1 and Sp3 is required for neuronal differentiation of N1E-115 cells. J. Biol. Chem. *277*, 11904–11909.

Yoshida, Y. *et al.* (2004). The stimulatory action of amphiphysin on dynamin function is dependent on lipid bilayer curvature. EMBO J *23*, 3483–3491.

Zelhof, A. C., and Hardy, R. W. (2004). WASp is required for the correct temporal morphogenesis of rhabdomere microvilli. J. Cell Biol. *164*, 417–426.

Zhang, J., Liu, X., Scherer, D. C., van Kaer, L., Wang, X., and Xu, M. (1998). The 40-kDa subunit of DNA fragmentation factor induces DNA fragmentation and chromatin condensation during apoptosis. Proc. Natl. Acad. Sci. USA *95*, 8461–8466.

The EMBO Journal (2007) 26, 2981–2990 | © 2007 European Molecular Biology Organization | All Rights Reserved 0261-4189/07
www.embojournal.org

THE EMBO JOURNAL

Truncations of amphiphysin I by calpain inhibit vesicle endocytosis during neural hyperexcitation

Yumei Wu[1], Shuang Liang[2], Yoshiya Oda[3], Iori Ohmori[1], Tei-ichi Nishiki[1], Kohji Takei[2], Hideki Matsui[1] and Kazuhito Tomizawa[1,*]

[1]Department of Physiology, Okayama University Graduate School of Medicine, Dentistry and Pharmaceutical Sciences, Okayama, Japan, [2]Department of Neuroscience, Okayama University Graduate School of Medicine, Dentistry and Pharmaceutical Sciences, Okayama, Japan and [3]Laboratory of Seed Finding Technology, Eisai Co., Ltd, Tsukuba, Japan

Under normal physiological conditions, synaptic vesicle endocytosis is regulated by phosphorylation and Ca^{2+}-dependent dephosphorylation of endocytic proteins such as amphiphysin and dynamin. To investigate the regulatory mechanisms that may occur under the conditions of excessive presynaptic Ca^{2+} influx observed preceding neural hyperexcitation, we examined hippocampal slices following high-potassium or high-frequency electrical stimulation (HFS). In both cases, three truncated forms of amphiphysin I resulted from cleavage by the protease calpain. *In vitro*, the binding of truncated amphiphysin I to dynamin I and copolymerization into rings with dynamin I were inhibited, but its interaction with liposomes was not affected. Moreover, overexpression of the truncated form of amphiphysin I inhibited endocytosis of transferrin and synaptic vesicles. Inhibiting calpain prevented HFS-induced depression of presynaptic transmission. Finally, calpain-dependent amphiphysin I cleavage attenuated kainate-induced seizures. These results suggest that calpain-dependent cleavage of amphiphysin I inhibits synaptic vesicle endocytosis during neural hyperexcitation and demonstrate a novel post-translational regulation of endocytosis.

The EMBO Journal (2007) **26**, 2981–2990. doi:10.1038/sj.emboj.7601741; Published online 31 May 2007
Subject Categories: neuroscience
Keywords: amphiphysin; calpain; endocytosis; hyperexcitation; seizure

Introduction

Clathrin-mediated endocytosis is the major mechanism for maintaining the synaptic vesicle recycling pool for synaptic transmission in small central synapses during repetitive high-frequency electrical stimulation (HFS) or even physiological stimulation (Granseth *et al*, 2006). Clathrin-mediated endocytosis consists of four steps: nucleation, invagination, fission and uncoating. Many endocytosis-related proteins are recruited to form complexes on the retrieved pits at each step after calcium-dependent calcineurin activity is activated by neural excitation. Amphiphysin I, a major dynamin-binding partner localized on the collar of retrieved vesicles, plays a key role in clathrin-mediated endocytosis of synaptic vesicles (Wigge and McMahon, 1998; Zhang and Zelhof, 2002; Evergren *et al*, 2004). Amphiphysin I mediates invagination and fission of synaptic vesicles, senses and facilitates membrane curvature via its BAR domain (Zhang and Zelhof, 2002; Peter *et al*, 2004) and stimulates the GTPase activity of dynamin in the presence of lipid membrane (Yoshida *et al*, 2004; Yoshida and Takei, 2005). The function of both amphiphysin I and dynamin is known to be regulated by phosphorylation and Ca^{2+}-dependent dephosphorylation (Slepnev *et al*, 1998; Cousin and Robinson, 2001; Tan *et al*, 2003; Tomizawa *et al*, 2003) under physiological conditions. Under resting conditions, endocytosis proteins such as amphiphysin I and dynamin are phosphorylated by Cdk5 (cyclin-dependent kinase 5). Once neural excitability is transferred to the nerve terminal, calcium influx to the presynaptic terminal occurs through VDCCs and activates phosphatase 2B calcineurin, which dephosphorylates the endocytic proteins. These proteins then form a complex and induce clathrin-mediated endocytosis.

Massive amount of Ca^{2+} enter presynaptic terminals during the neural hyperexcitation observed in neurodegenerative disorders such as ischemia/anoxia, epilepsy, stroke, trauma and Alzheimer's disease. Previous studies have shown that hyperexcitation, such as repetitive HFS or high potassium stimulation, at presynapses induces short-term depression at postsynapses in hippocampal neurons (Stevens and Wesseling, 1999; Sara *et al*, 2002). This short-term depression is thought to be a neuroprotective mechanism for protecting neurons from hyperexcitability. However, the mechanism of the short-term depression after Ca^{2+} influx is unclear. Previous studies have shown that synaptic vesicle endocytosis, which contributes to maintaining synaptic transmission, is inhibited during synaptic depression (Sun *et al*, 2002; Wu, 2004). These results suggest that inhibition of clathrin-mediated endocytosis may be involved in the short-term depression at mammalian synapses after excessive presynaptic Ca^{2+} influx.

Calcium-dependent calpain activity is increased by massive calcium influx, and promotes the degradation of key cytoskeletal and membrane proteins or cleavage of many other important proteins such as calcineurin in neuroexcitotoxicity (Wu *et al*, 2004; Czogalla and Sikorski, 2005), which has been shown to be related to various neurodegenerative disorders. Moreover, several presynaptic proteins such as spectrin (Saido *et al*, 1993), PKC (Sessoms *et al*, 1992) and p35 (Lee *et al*, 2000), a Cdk5 activator, are substrates of calpain. The function of these proteins may be affected by calpain cleavage. In the present study, we found that the important endocytosis protein amphiphysin I is cleaved by

*Corresponding author. Department of Physiology, Okayama University Graduate School of Medicine, Dentistry and Pharmaceutical Sciences, Shikata-cho 2-5-1, Okayama 700-8558, Japan. Tel.: +81 86 235 7107; Fax: +81 86 235 7111; E-mail: tomikt@md.okayama-u.ac.jp

Received: 19 April 2007; accepted: 8 May 2007; published online: 31 May 2007

calpain during high potassium stimulation, repetitive high-frequency stimulation and kainate (KA)-induced seizures. Calpain-cleaved amphiphysin I lost its function of binding with dynamin *in vitro*, and overexpression of the truncated form of amphiphysin I in COS-7 cells and neurons inhibited clathrin-mediated endocytosis. Inhibition of clathrin-mediated endocytosis of synaptic vesicles by calpain-dependent amphiphysin I cleavage is involved in repetitive HFS-induced synaptic depression and KA-induced seizures.

Results

High K^+ induces multiple amphiphysin I cleavages by calpain in mouse hippocampal slices

We first investigated whether amphiphysin I was cleaved under conditions of excessive Ca^{2+} influx into nerve terminals (80 mM KCl) or under neurotoxic conditions (500 μM L-glutamate) in the hippocampal slices. In both cases, three major truncated products of amphiphysin I were detected by Western blotting analysis using anti-amphiphysin I antibodies recognizing the N terminus (Figure 1A). The antibodies reacted with 52, 47 and 43-kDa proteins on SDS–PAGE gels. The induction of these truncations was greater with high potassium (high K^+) stimulation than with glutamate stimulation (Figure 1A). Moreover, a weak fourth band of amphiphysin I was sometimes detected in the hippocampal slices given high K^+ stimulation (arrow in Figure 1A). These results suggest that excessive Ca^{2+} influx in presynaptic terminus may induce the cleavage of amphiphysin I. The Ca^{2+}-dependent cysteine protease calpain is involved in various neurological processes, and an increase in calpain activity is related to the pathophysiology of neurodegenerative disorders such as neuroexcitotoxicity and ischemia (Rami, 2003; Wu *et al*, 2004). We therefore examined whether calpain is involved in the cleavage of amphiphysin I after high K^+ stimulation. Figure 1B shows the time-dependent cleavages of amphiphysin I and α-spectrin, a physiological substrate of calpain, in hippocampal slices after high K^+ stimulation. Amphiphysin I was rapidly cleaved with obvious truncations observed 30 s after the stimulation (Figure 1B), and 41% of amphiphysin I was cleaved 20 min after the stimulation. α-Spectrin was also rapidly cleaved after high K^+ stimulation and was more extensively cleaved than amphiphysin I after 20 min of stimulation (Figure 1B). Subcellular fractionation showed that two isoforms of calpain, μ- and m-calpain, existed in the membrane and cytosol fractions of purified synaptosomes (LP2 and LS2 fractions in Figure 1C). Two potent calpain inhibitors, ALLM and ALLN, inhibited the high K^+-induced truncations of amphiphysin I in the hippocampal slices (Figure 1D). Moreover, m-calpain cleaved recombinant amphiphysin I *in vitro*, yielding three truncated forms with molecular masses equal to those of the truncated forms observed in hippocampal slices after high K^+ stimulation (Figure 1E). A high concentration (40 nM) of m-calpain almost completely cleaved amphiphysin I to the 43-kDa form, and 52-kDa amphiphysin I was not observed (Figure 1E). We also examined the effect of μ-calpain on amphiphysin I cleavage *in vitro* (Supplementary Figure 1). μ-Calpain cleaved amphiphysin I to the same three major truncated forms as m-calpain, and in addition to one new truncated form between the 52 and 47-kDa forms. These

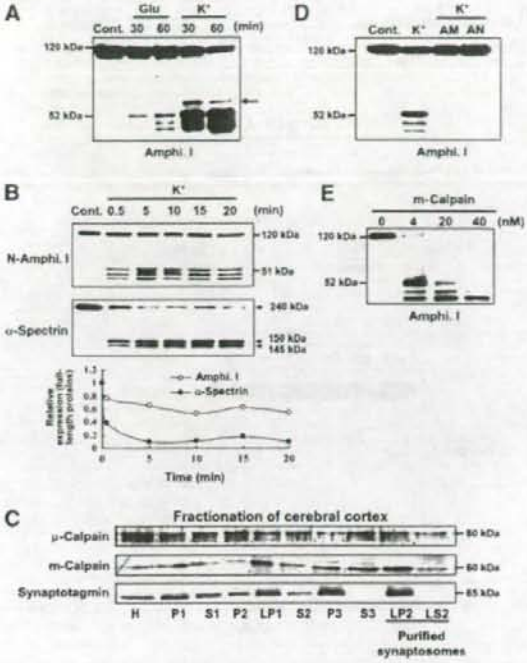

Figure 1 High K^+ induces multiple amphiphysin I (Amphi. I) cleavages by calpain in mouse hippocampal slices. (**A**) Western blotting analysis of hippocampal slices stimulated with L-glutamate or high K^+ and then allowed to rest for the indicated times. Probing with anti-amphiphysin I antibody recognizing the N terminus demonstrated the presence of three truncated forms of amphiphysin I. Arrow, fourth truncated form of amphiphysin I. (**B**) Time-dependent cleavages of amphiphysin I and α-spectrin after high K^+ stimulation of hippocampal slices for the indicated times. The lowest panel shows the quantitative analysis of the expression changes of FL amphiphysin I and α-spectrin after high K^+ stimulation. The expression levels of both proteins of the control (time-0 min) were set at 1. (**C**) Subcellular fractionation of μ- and m-calpain from cerebral cortex as shown by probing with anti-μ- and m-calpain antibodies. Anti-synaptotagmin antibodies were used to monitor synaptosomal fractions. H, total homogenate; P2, crude synaptosomal pellet; LP2, membrane fraction of purified synaptosomes; LS2, cytosol fraction of purified synaptosomes. (**D**) Anti-amphiphysin I immunoblotting showing that calpain inhibitors, ALLM (AM) or ALLN (AN), blocked high K^+-induced amphiphysin I cleavage. (**E**) Anti-amphiphysin I immunoblotting showing the *in vitro* cleavage of recombinant amphiphysin I (0.5 μg/μl) by various concentrations of recombinant m-calpain.

results suggest that amphiphysin I may be cleaved by calpain during neural hyperexcitation.

Identification of the cleavage sites of amphiphysin I by calpain

To determine whether calpain cleaved the N- or C terminus of amphiphysin I, two different anti-amphiphysin I antibodies (designated antibody I and II), which recognized the N- and the C terminus, respectively, were used to detect the truncations *in vitro* (Figure 2A). Antibody I detected three truncated forms (Figure 2A). In contrast, antibody II detected a truncated form of amphiphysin I with molecular mass of 76 kDa. CBB staining showed three truncations of amphiphysin I and the molecular masses of the truncations on SDS–PAGE agreed

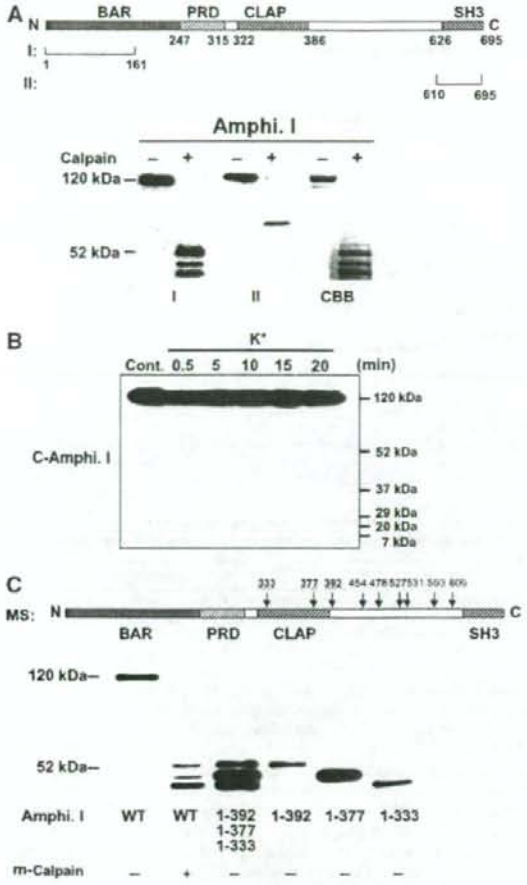

Figure 2 Sites of cleavage of amphiphysin I by calpain. (**A**) Upper panel, schematic diagram of human amphiphysin I and the recognition sites of each anti-amphiphysin I antibody (recognizing the N terminus (I) or C terminus (II)). Lower panel, Western blotting showing the m-calpain (7 nM)-induced truncation products of recombinant amphiphysin I recognized by anti-amphiphysin I antibodies I and II. CBB staining showing amphiphysin I was mainly cleaved to three fragments corresponding to the truncated products detected by antibody I. (**B**) No truncated form of amphiphysin I was detected by antibody II in high K^+-treated hippocampal slices. (**C**) Three major truncations of amphiphysin I. Upper panel, scheme of the cleavage sites by m-calpain identified by MS analysis. Lower panel, comparison of the molecular weights of amphiphysin I cleaved *in vitro* by m-calpain with those of the recombinant proteins of each truncation form identified by MS.

with those of amphiphysin I truncations detected with antibody I. However, obvious truncations of amphiphysin I corresponding to the 76-kDa form was not observed on CBB-stained gels. Moreover, antibody II did not detect any truncated forms in the hippocampal slices after high K^+ stimulation (Figure 2B). These results suggest that the truncated forms of amphiphysin I are N-terminal fragments, and C-terminal fragments may be degraded after high K^+ stimulation. The precise cleavage sites of amphiphysin I were identified by mass spectrometric analysis (MS). Interestingly, MS showed that the protein was cleaved at nine sites of the C terminus (positions 333, 377, 392, 454, 478, 527, 531, 593 and 609) (Figure 2C and Supplementary Figures 2 and 3). Figure 2C shows a comparison of the molecular weights of the truncated forms of amphiphysin I cleaved *in vitro* by calpain and the recombinant proteins of each truncated form (1–333, 1–377 and 1–392) identified by MS. The molecular weights of the cleaved forms of amphiphysin I agreed with those of the recombinant proteins. These results suggest that positions 333, 377 and 392 correspond to the truncation sites after high K^+ stimulation among the cleavage sites identified by MS.

Interaction of amphiphysin I with liposomes and dynamin I inhibits the cleavage by calpain

Amphiphysin I is associated with synaptic plasma membrane through the BAR domain (Zhang and Zelhof, 2002; Peter *et al*, 2004). This phenomenon can be reconstituted as a tubulation of liposomes in a cell-free system (Figure 3A). Moreover, the protein binds dynamin I via the SH3 domain and coassembles with dynamin I into rings either in solution or on lipid tubules (Figure 3A). We examined whether the association of amphiphysin I with liposomes and/or dynamin I affected the truncations by calpain. Amphiphysin alone was completely cleaved to three truncated forms by calpain (Figure 3B, lane 5). In contrast, amphiphysin I bound to liposomes was resistant to cleavage by calpain regardless of the binding with dynamin I (Figure 3B, lanes 2 and 3). Interaction with dynamin I inhibited the production of two of the truncated forms of amphiphysin I with molecular masses of 47 and 43 kDa (Figure 3B, lane 6). On the other hand, dynamin I was not cleaved by calpain under various conditions (Figure 3C). To investigate whether liposomes influenced calpain activity, calpain cleavage of calcineurin, a good substrate of calpain (Wu *et al*, 2004), was examined in the presence of liposomes. Calpain cleaved calcineurin as efficiently in the presence of liposomes as in their absence, suggesting that liposomes have no effect on calpain activity (Figure 3D). These results suggest that the association of amphiphysin I with synaptic membranes and dynamin may be crucial for the regulation of its cleavage by calpain. The interaction of amphiphysin I with dynamin I is strictly regulated by phosphorylation and dephosphorylation (Tomizawa *et al*, 2003; Liang *et al*, 2007). Phosphorylation of amphiphysin I by Cdk5 inhibits the interaction with endocytic proteins, whereas calcineurin-dependent dephosphorylation of amphiphysin I induces this interaction (Tomizawa *et al*, 2003). It was next examined whether calpain-dependent cleavage of amphiphysin I was regulated by phosphorylation and dephosphorylation. A phospho-mimic mutant of amphiphysin I (5D) in which five sites (S261, S272, S276, S285 and T310) phosphorylated by Cdk5 were replaced with Asp was cleaved by m-calpain the same way as dephospho-amphiphysin I *in vitro* (Figure 3E). However, preincubation with FK506, a potent calcineurin inhibitor, increased the levels of high K^+-stimulated amphiphysin I cleavages in hippocampal slices compared with roscovitine, a potent Cdk5 inhibitor (Figure 3F). These results suggest that phosphorylation of amphiphysin I does not directly influence the cleavage of amphiphysin I by calpain, but that the phosphorylation inhibits the formation of a complex with endocytic proteins and synaptic vesicle membranes, resulting in the induction of cleavage of amphiphysin I by calpain during hyperexcitation.

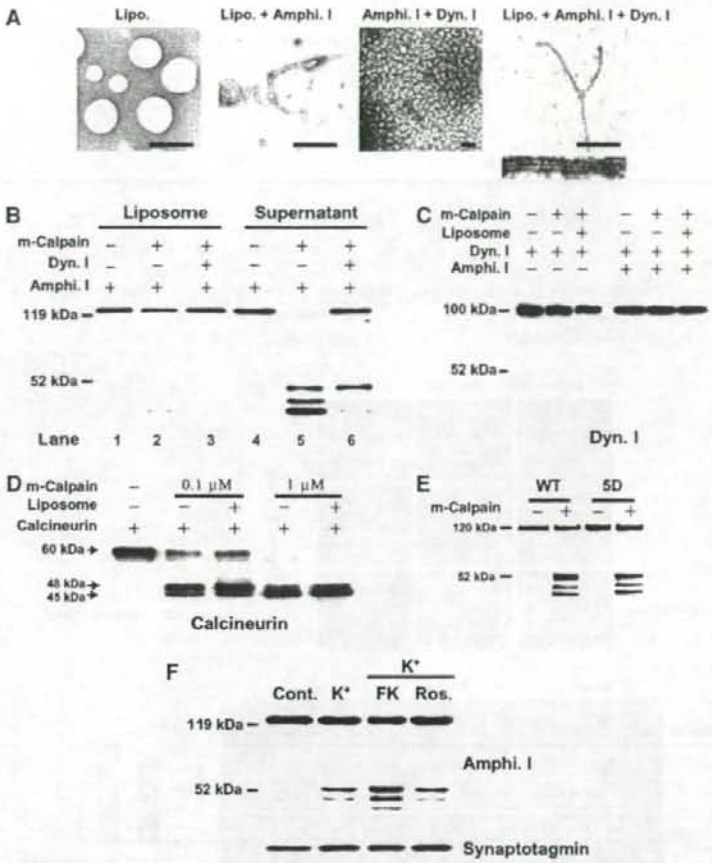

Figure 3 Interaction of amphiphysin I (Amphi. I) with liposomes and dynamin I (Dyn. I) inhibits the cleavage by calpain. (**A**) Morphological analysis of the interaction of amphiphysin I with liposomes and dynamin I at the electron microscopic level. Amphiphysin I recruits dynamin I onto liposomes, forming collars on tubulated liposomes. Bars in upper panels, 2 μm, bar in lower panel, 100 nm. (**B**) Effects of the interaction of amphiphysin I with liposomes and dynamin I on its cleavage by calpain are shown by anti-amphiphysin I immunoblotting of liposome and liposome-free fractions of the incubation mixture. (**C**) Anti-dynamin I immunoblotting shows that dynamin I was not cleaved by calpain in the presence or absence of either liposomes or amphiphysin I. (**D**) The effect of liposomes on calpain activity was examined by incubating purified calcineurin in the presence or absence of liposomes. Calcineurin cleavage by calpain was examined by Western blotting with anti-calcineurin antibodies. (**E**) Comparison of calpain-dependent cleavage between WT amphiphysin I and its phospho-mimic mutant form *in vitro*. For the mutant, Cdk5 phosphorylation sites (S261, S272, S276, S285 and T310) of amphiphysin I were replaced with Asp (5D). Both types of recombinant amphiphysin I were incubated with 2 nM m-calpain for 30 min. (**F**) The effect of phosphorylation of amphiphysin I on its cleavage by calpain was examined in hippocampal slices treated with either FK506 (FK), an inhibitor of calcineurin, or roscovitine (Ros.), a Cdk5 inhibitor. Hippocampal slices were preincubated with and without 50 μM FK or 10 μM Ros. for 30 min at 30°C and were then treated with 80 mM KCl for 15 min. Homogenized slices were analyzed by immunoblotting with anti-amphiphysin I and anti-synaptotagmin antibodies.

Amphiphysin I cleaved by calpain and a truncated form (1–392) are capable of tubulation with liposomes, but do not form ring structures with dynamin I

To investigate whether calpain-dependent cleavage of amphiphysin I affects its function, the interactions of amphiphysin I with liposomes and dynamin I were examined *in vitro* (Figure 4). Liposomes formed tubules with cleaved amphiphysin I (Figure 4Ac) just as they did with full-length (FL) amphiphysin I (Figure 4Aa). Recombinant protein corresponding to one of the truncated forms (1–392) also underwent tubule formation with liposomes (Figure 4Ad). These results suggest that amphiphysin I cleaved by calpain may be capable of binding to synaptic membranes. On the other hand, amphiphysin I cleaved by calpain (Figure 4Ag) or the recombinant protein corresponding to the truncated form (Figure 4Ah) did not form ring structures with dynamin I, whereas FL amphiphysin I did form small rings (Figure 4Ae and f). Moreover, when incubated with liposomes and dynamin I, the truncated form failed to form the thick helical collars on tubules (Figure 4Aj), which are formed with FL amphiphysin I (Figure 4Ai). These results indicate that calpain-dependent truncation of amphiphysin I inhibits the interaction with dynamin I. Since both dynamin ring structures and thick helical collars on tubules are required for the formation of endocytic synaptic vesicles, our findings suggest that both of these processes are inhibited following calpain cleavage of amphiphysin I during hyperexcitation.

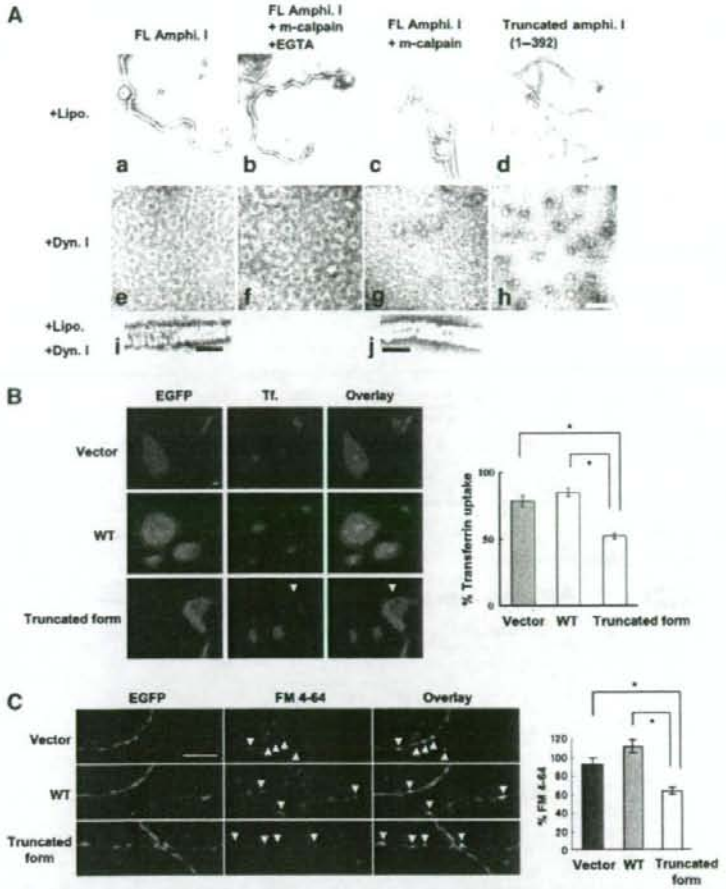

Figure 4 Amphiphysin I cleaved by calpain and a truncated form (1–392) are capable of tubulation with liposomes, but do not form ring structures with dynamin I (**A**: a–j), and inhibitory effect of calpain-dependent truncated form of amphiphysin I on transferrin uptake in Cos-7 cells (**B**) and FM 4–64 labeling in primary culture of hippocampal neurons (**C**). (A: a–d) The effect of truncation on the ability of amphiphysin I to form tubules with liposomes. As a chelator of Ca^{2+}, EGTA inhibits calpain activity. (A: e–h) The effect of both forms of amphiphysin I on the formation of ring structures with dynamin I. (A: i, j) Comparison of helical collars on the tubules of FL and truncated amphiphysin I when incubated with dynamin I plus liposomes. Bars in A: d and h, 500 nm; bars in A: i and j, 100 nm. (B) Confocal laser scanning micrographs of: left panel, EGFP expression on COS-7 cells transfected with pIRES2-EGFP vector only (Vector), the vector containing wild-type amphiphysin I cDNA (WT) and the vector containing truncated amphiphysin I (1–392) cDNA (truncated form); middle panel, transferrin (Tf.) uptake in similarly transfected cells exposed to transferrin 24 h later; and, right panel, showing the overlay of EGFP and transferrin uptake. Transferrin uptake was inhibited in cells transfected with truncated amphiphysin I (arrows); bar, 10 μm. For quantification of the results, transferrin uptake was calculated as the mean fluorescence density for 315–660 cells under each condition and the mean values (±s.e.m.) were expressed as a percentage of normal transferrin uptake in untransfected cells. $^*P<0.01$. (C) Fluorescence imaging micrographs of: left panel, EGFP expression on presynapses of neurons transfected with vector, WT amphiphysin I and the truncated form (amphi. 1–392); middle panel, subtracted images of FM 4–64 (loading minus unloading); right panel showing overlay of EGFP expression and FM 4–64 labeling. Bar, 10 μm. FM 4–64 labeling was inhibited in boutons transfected with truncated amphiphysin I (arrows). Right graph shows the results of quantitative analysis. FM 4–64 labeling was calculated as the integral fluorescence intensity for 47–55 boutons under each condition and the mean values (±s.e.m.) were expressed as a percentage of normal FM 4–64 labeling in untransfected boutons. $^*P<0.01$.

We further investigated whether calpain-dependent cleavage of amphiphysin I influenced clathrin-mediated endocytosis in cells. Wild-type (WT) amphiphysin I and one of its truncated forms (1–392) were overexpressed in Cos-7 cells, and transferrin uptake in the cells was examined (Figure 4B). Transferrin uptake in the truncated amphiphysin I-overexpressing cells was inhibited by 61% compared to that in WT amphiphysin I-overexpressing cells (Figure 4B). Moreover, the results were confirmed in rat hippocampal neurons. We investigated whether calpain-dependent cleavage of amphiphysin I affected presynaptic vesicle endocytosis in rat hippocampal neurons. FM 4–64 labeling in the truncated amphiphysin I-overexpressing boutons was inhibited by 57% compared to that in WT amphiphysin I-overexpressing boutons. These results indicate that calpain-dependent cleavage of amphiphysin I inhibits clathrin-mediated synaptic vesicle endocytosis.

Amphiphysin I cleavage by calpain inhibits excessive synaptic transmission in hippocampal slices and in vivo

Repetitive, high-frequency electrical nerve stimulation (e.g., 10 Hz) causes short-term synaptic depression in hippocampal

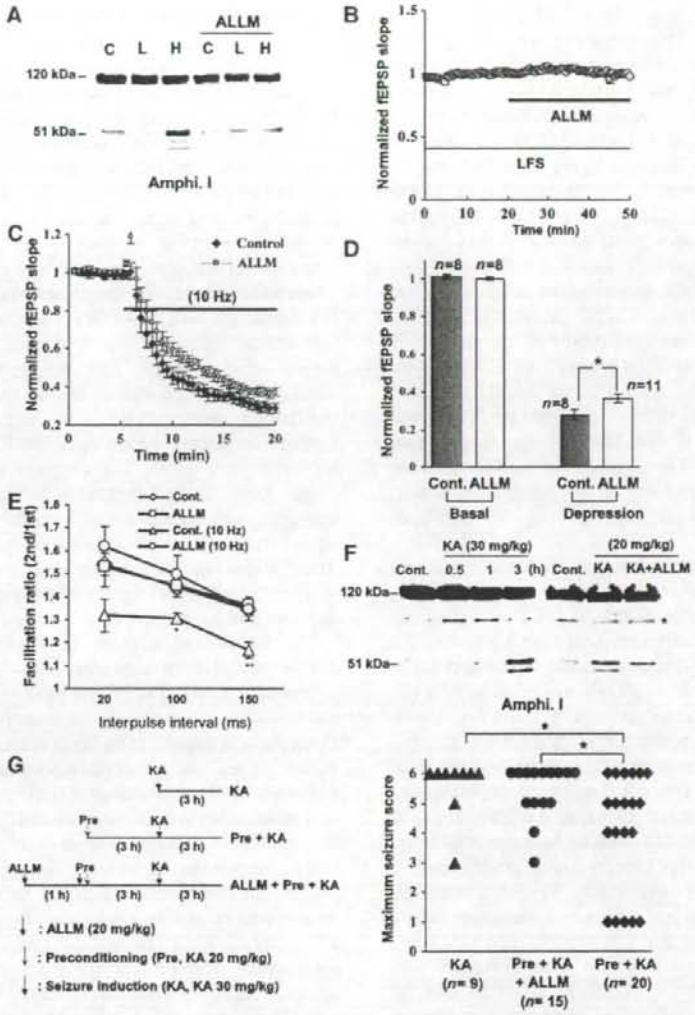

Figure 5 Amphiphysin I cleavage by calpain inhibits excessive synaptic transmission in hippocampal slices and *in vivo*. (**A**) Anti-amphiphysin I immunoblot showing the effects of either no electrical stimulation (C), LFS (L, 0.03 Hz) or HFS (H, 10 Hz) on calpain-dependent amphiphysin I cleavage in mouse hippocampal slices, without or with ALLM preincubation. (**B**) ALLM inhibition of calpain had no effect on fEPSP slope during LFS. (n = 7) (**C**) Effect of calpain inhibition (ALLM) on fEPSP depression induced by HFS. Control, $n = 8$; ALLM, $n = 11$. (**D**) Comparison of fEPSP slopes at 15 min after LFS and HFS in the ALLM-perfused slices and controls. $^*P < 0.05$. (**E**) PPF in hippocampal slices following LFS is reduced following HFS, an effect that is blocked by inhibiting calpain with ALLM. ALLM had no effect on PPF following LFS. The data represent the ratios of the second EPSP slopes versus the first fEPSP slopes separated by the given intervals. As a control, hippocampal slices were incubated with DMSO instead of ALLM. $^*P < 0.05$, $^{**}P < 0.01$ compared with Cont. $n = 10$–15. (**F**) Anti-amphiphysin I immunoblot showing the ability of KA injections to induce calpain-dependent amphiphysin I cleavage in the hippocampus of FVB/NJ mice. Preincubation with ALLM inhibited the KA-induced cleavage of amphiphysin I. *Nonspecific band. (**G**) Preconditioning with low-dose KA prevented KA-induced development of seizures in the FVB/NJ mice and ALLM inhibited the preconditioning effect. Left panel, schematic time schedule of the animal experiments. Right panel, the maximum seizure score in mice of each group. Seizure scores were monitored for 3 h after KA (30 mg/kg) injection as described in 'Methods'. $^*P < 0.05$.

neurons and neuromuscular junctions (Figure 5C and Wu and Betz, 1998) mainly because synaptic vesicles are depleted (Wang and Kaczmarek, 1998). Clathrin-mediated endocytosis is inhibited during frequency-dependent depression, resulting in the depletion of the recycling pool of synaptic vesicles (Wu and Betz, 1998; Wu, 2004). These data along with the present results led us to hypothesize that amphiphysin I is cleaved by calpain during HFS, and that the cleavage causes high frequency-induced depression of synaptic transmission through the inhibition of clathrin-mediated endocytosis. To test this hypothesis, we examined whether calpain-dependent cleavage of amphiphysin I was involved in the depression of the field EPSP (fEPSP) at the synapses from Schaffer collaterals onto CA1 pyramidal cells in hippocampal slices. HFS (10 Hz) induced amphiphysin I cleavage, whereas low-frequency stimulation (LFS, 0.03 Hz) produced no

cleavage (Figure 5A). Blocking calpain with ALLM inhibited the HFS-induced cleavages. Thus, calpain cleaves amphiphysin I during repetitive HFS in hippocampal slices. Perfusion of ALLM for 30 min had no effect on fEPSP slope when slices were stimulated with LFS (Figure 5B). In contrast, ALLM inhibited HFS-induced fEPSP depression (Figure 5C and D). To clarify whether the effect of calpain inhibition on the fEPSP depression is exerted in the presynapse or in the postsynapse, the effect of ALLM on paired-pulse facilitation (PPF) was examined in hippocampal slices. PPF is a transient form of presynaptic plasticity, in which the second of two closely spaced stimuli elicits enhanced transmitter release, because of residual calcium ions in the presynaptic terminal after the first stimulus (Zucker, 1989). PPF at 100 and 150 ms interpulse intervals was decreased after HFS (10 Hz) compared with that after LFS (Figure 5E). In the ALLM-treated slices, in contrast, PPF after HFS was not decreased compared with that after LFS (Figure 5E). These results suggest that cleavages of amphiphysin I by calpain may partially account for the HFS-induced depression of synaptic transmission through the inhibition of clathrin-mediated endocytosis of synaptic vesicles.

Excessive synaptic activity is the primary cause of seizures and seizure-induced brain damage, and many drugs inhibiting the neurotransmitter release machinery in epileptogenic areas are thought to be effective anti-ictal agents (Okada *et al*, 2002; Costantin *et al*, 2005). Intraperitoneal injection of KA in FVB/NJ mice induces limbic motor seizures originating in the hippocampus (Lothman and Collins, 1981; Ben-Ari, 1985). Finally, we investigated whether amphiphysin I was cleaved by calpain during hyperexcitation in the hippocampus of KA-injected FVB/NJ mice. Obvious cleavage of amphiphysin I was observed 3 h after 30 and 20 mg/kg KA injection, and administration of ALLM inhibited the KA-induced amphiphysin I cleavage, suggesting that calpain cleaves amphiphysin I during hyperexcitation *in vivo* (Figure 5F). To clarify the physiological function of amphiphysin I cleavage during neural hyperexcitation, the effect of amphiphysin I cleavage on KA-induced seizure development was examined. KA injection (30 mg/kg) induced seizure behavior in FBV/NJ mice (Figure 5G). The maximum seizure score was stage 6 in almost all KA-injected mice (75%) (Figure 5G). Preconditioning with low-dose KA injection (20 mg/kg) induced amphiphysin I cleavages in the mice (Figure 5F). Preconditioning 3 h before KA injection (30 mg/kg) reduced the KA-induced seizure development (Figure 5G), so that only 30% of the mice developed stage 6 seizures. Moreover, administration of ALLM attenuated the preconditioning effect, so that 60% of the mice developed stage 6 seizures (Figure 5G). These results suggest that amphiphysin I may be cleaved by calpain during neural hyperexcitation *in vivo* and the cleavage may inhibit excessive neurotransmitter release.

Discussion

In the present study, we found a novel posttranslational regulation of an endocytic protein, amphiphysin I, during neural hyperexcitation. Phosphorylation and dephosphorylation of endocytic proteins are well-known post-translational regulatory mechanisms involved in clathrin-mediated endocytosis in the normal physiological state (Cousin and Robinson, 2001). In contrast, the present results showed that amphiphysin I was not cleaved by calpain under normal physiological conditions. The protein was cleaved during neural hyperexcitation and its cleavage was regulated by its interaction with other endocytic proteins or the cell membrane. We showed that amphiphysin I is cleaved by calpain during high potassium-induced hyperexcitation in rat hippocampal slices, and the cleavage blocked the interaction of amphiphysin I with dynamin I, a key molecule in the fission of clathrin-coated buds from presynaptic membrane through its GTPase activity, *in vitro*. In addition, the N-terminal fragments of amphiphysin I still retained the ability to bind to liposome membranes after the calpain proteolysis, suggesting a dominant-negative effect of amphiphysin I cleavage by calpain on clathrin-mediated synaptic vesicle endocytosis during hyperexcitation. This was proven by the inhibition of clathrin-mediated endocytosis of transferrin and synaptic vesicles by overexpression of the amphiphysin I truncation product containing amino acids 1–392 in Cos-7 cells and hippocampal neurons. The cleavage of amphiphysin I by calpain is an irreversible process, in contrast to phosphorylation and dephosphorylation. Therefore, the dysfunction of amphiphysin I and its dominant-negative effect resulting from the cleavage are maintained for a long period, resulting in long-lasting inhibition of clathrin-mediated endocytosis and synaptic transmission.

The function of cleavage of amphiphysin I by calpain during neural hyperexcitation may be to inhibit neural hyperexcitability and to protect neurons from neural damage and neuronal cell death. Although the role of synaptic vesicle endocytosis is thought to be to maintain the recycling synaptic vesicle pool for exocytosis during repetitive high-frequency nerve stimulation, previous studies have shown that endocytosis is inhibited during high-frequency stimulation-induced depression (Sun *et al*, 2002; Wu, 2004). These results suggest that the synaptic depression induced by some presynaptic mechanisms may be important for neuronal auto-protection against neural hyperexcitation, and inhibition of synaptic vesicle endocytosis may play a part in the mechanism. The present study showed that cleavage of amphiphysin I by calpain was induced by HFS in hippocampal slices, and ALLM inhibited the HFS-induced fEPSP depression and blocked the depression-induced inhibition of PPF. We further confirmed this phenomenon *in vivo*. Preconditioning with low-dose KA induced calpain-related amphiphysin I cleavage and reduced the development of seizures in FVB/NJ mice. However, administration of ALLM attenuated the preconditioning effect. Although *in vivo* studies did not directly show that calpain regulated assembly of the fission complex of clathrin-mediated synaptic vesicles during hyperexcitation, these results suggest that hyperexcitation-induced amphiphysin I cleavage may play a role in fEPSP depression, which is thought to be a neuroprotective mechanism. Taken together, both the *in vivo* and *in vitro* studies showed that hyperexcitation-induced amphiphysin I cleavage plays a role in protecting neurons from neuroexcitotoxicity during hyperexcitation.

There is an SH3 domain in the C terminus of amphiphysin I. The SH3 domain is a potent inhibitor of synaptic vesicle endocytosis (Shupliakov *et al*, 1997). We first speculated that the calpain cleavage-dependent C-terminal fragment of amphiphysin I was involved in the inhibition of synaptic vesicle endocytosis during hyperexcitation. However, antibody II did

not detect any C-terminal fragments of amphiphysin I. Moreover, MS identified nine sites in the C terminus of amphiphysin I as the cleavage sites targeted by calpain. These results suggest that amphiphysin I may undergo multiple cleavages at the C terminus by calpain, and that the C-terminal fragments are rapidly degraded after the cleavage. Finally, the three N-terminal fragments remain and inhibit synaptic vesicle endocytosis through the inhibition of the interaction with synaptic membranes and dynamin.

Both m- and μ-calpain were expressed in the presynaptic terminus. *In vitro* cleavage studies showed that m-calpain cleaved amphiphysin I to three fragments corresponding to the truncations observed in high K^+-treated hippocampal slices. In contrast, μ-calpain cleaved the protein to four fragments. These results suggest that m-calpain may be involved in amphiphysin I cleavage during neural hyperexcitation.

A number of previous studies showed that changes in calpain activity are related to the pathophysiology of neurodegenerative disorders, such as neuroexcitotoxicity, cerebral ischemia and traumatic brain injury (Posmantur *et al*, 1996; Rami, 2003; Wu *et al*, 2004). The elevation of intracellular Ca^{2+} levels during the course of injuries and diseases of the central nervous system causes overactivation of calpain, promoting degradation of key cytoskeletal and membrane proteins, and leading to neuronal cell death (Czogalla and Sikorski, 2005). To date, the key proteins shown to be cleaved by calpain are localized in the postsynapse. Although the reason for the difference in calpain function presynapse versus postsynapse during neural hyperexcitation remains unclear, specific inhibition of calpain in the postsynapse may exert a potent neuroprotective effect.

Materials and methods

Western blotting analysis

Monoclonal anti-amphiphysin I antibodies (I and II) were provided by P De Camilli (Yale University, New Haven, CT). Monoclonal anti-amphiphysin I antibody recognizing the N terminus was purchased from Lab Frontier (LF-MA0047, Seoul, Korea). Polyclonal anti-μ-calpain antibody was from Merck (San Diego, CA), monoclonal anti-m-calpain antibody was from Sigma-Aldrich (Clone 107–82, St Louis, MO), polyclonal anti-calcineurin A antibody was from StressGen Biotech (SPA-610, Victoria, BC, Canada), the polyclonal anti-α-spectrin II antibody was from Santa Cruz Biotechnology (Sc-7465, Santa Cruz, CA); the monoclonal anti-synaptotagmin I antibody was from BD Transduction Laboratories (S39520, San Jose, CA) and polyclonal anti-dynamin I antibody was from Santa Cruz Biotechnology (Sc-6402). Western blotting analysis was performed as described previously (Tomizawa *et al*, 2002). After incubation with the appropriate secondary antibody conjugated with horseradish peroxidase (Sigma-Aldrich), positive bands were visualized using an enhanced chemiluminescence detection system (Amersham Biosciences, Pittsburgh, PA).

Preparation of hippocampal slices and electric stimulation

Hippocampal slices was prepared as described previously (Tomizawa *et al*, 2002). Briefly, the hippocampi of male C57BL/6 mice aged 7–8 weeks were dissected, and 300–350 μm transverse slices were prepared. For high K^+ stimulation, after equilibration for more than 2 h at room temperature in oxygenated (95% O_2, 5% CO_2) ACSF solution containing (in mM): 125 NaCl, 26 $NaHCO_4$, 11 glucose, 2.5 KCl, 1.25 NaH_2PO_4, 2 $CaCl_2$, 1.3 $MgSO_4$, slices were treated with 80 mM potassium solution containing (in mM): 47.5 NaCl, 26 $NaHCO_4$, 11 glucose, 80 KCl, 1.25 NaH_2PO_4, 2 $CaCl_2$, 1.3 $MgSO_4$ at 32°C. For glutamate stimulation, the slices were incubated with ACSF in the presence of 500 μM L-glutamate (Sigma-Aldrich) for 15 min. The slices were then washed with ACSF and were further incubated for 15 or 45 min. After the reaction, the slices were sonicated in 1% SDS and then boiled for 3 min before Western blot analysis. For calpain inhibition studies, slices were preincubated in either 50 μM ALLM (AM) or ALLN (AN) for 30 min and then stimulated with high K^+ in the presence of ALLM or ALLN for 15 min. A Panasonic MED 64 System (Alpha MED Sciences, Osaka, Japan) was used for electrical stimulation. After equilibration for more than 2 h at room temperature, the slices were transferred to the MED probe and fixed with a slice anchor. The slices were stimulated along the Schaffer collaterals and field excitatory postsynaptic potentials (fEPSPs) were recorded in CA1. The intensity of the stimulation was adjusted to produce an fEPSP with a slope of 30–40% of the maximum. For Western blotting analysis, the CA1 region was cut out of the slices and sonicated in 1% SDS buffer.

Preparation of recombinant amphiphysin I and its truncated constructs, and purification of dynamin I

The cDNAs encoding FL human amphiphysin I and its truncation constructs corresponding to amino-acid sequences 1–333, 1–377 and 1–392 were prepared by PCR amplification using specific primers. FL and truncated forms of amphiphysin I cDNAs were subcloned into pGEX-6P vector as *Bam*HI–*Eco*RI fragments. The expression of GST-fusion proteins was induced by 0.1 mM isopropyl-1-thio-D-galactopyranoside at 25°C for 12 h in LB medium supplemented with 100 μg/ml ampicillin at $A_{600} = 0.8$. The purification of GST-fusion proteins was performed as described previously (Yoshida *et al*, 2004), and the cleavage of GST with PreScission protease was carried out according to the manufacturer's instructions. Finally, the protein was purified on a Mono Q column equilibrated in 20 mM Tris–HCl (pH 7.7) and 0.2 M NaCl. The protein solution was stored at −80°C, and thawed at 37°C before use.

Dynamin I was purified from bovine brain essentially as described previously (Liu *et al*, 1994).

Preparation of synaptosomes

Synaptic fractions were prepared from 7-week-old Wistar rat brains as described previously (Tomizawa *et al*, 2002). Expression of calpain I (μ-) and II (m-) in each fraction was analyzed by Western blotting analysis using specific antibodies.

Preparation of liposomes

Unilamellar liposomes in 0.3 M sucrose (1 mg/ml) were prepared as described previously (Takei *et al*, 1999).

In vitro proteolysis of amphiphysin I by calpain

Recombinant amphiphysin I (0.5 μg/μl) was incubated with 4–40 nM recombinant m-calpain (Merck) in reaction buffer (50 μl) containing 40 mM Tris–HCl (pH 7.5), 12 mM $CaCl_2$ at 25°C for 30 min. The reaction was stopped by the addition of SDS–PAGE sample buffer, and the reaction mixture was then separated by electrophoresis on a 10% SDS–PAGE gel. The cleavage of amphiphysin I was analyzed by Western blotting with monoclonal anti-amphiphysin I antibody recognizing the N terminus. To investigate the effect of amphiphysin I interaction with liposome or dynamin I on calpain-dependent amphiphysin I cleavage, 0.3 μg/μl liposome or dynamin I was incubated with 0.3 μg/μl amphiphysin I in 20 μl of cytosolic buffer containing 25 mM HEPES–KOH (pH 7.2), 25 mM KCl, 2.5 mM magnesium acetate, 100 mM potassium L-glutamate at 37°C for 15 min, and 7 nM calpain and 12 mM $CaCl_2$ were then added and the mixture was further incubated for 30 min at 25°C. The reaction mixture was then centrifuged at 20 600 *g* for 10 min, and the proteins in the pellet (liposome fraction) and the supernatant (liposome-free fraction) were analyzed by Western blotting with anti-N-terminal amphiphysin I and anti-dynamin I antibodies.

Mass spectrometry

Mass spectrometry was performed as described previously (Wu *et al*, 2004). Briefly, standard peptides, angiotensin III and oxidized insulin B chain, were obtained from Sigma-Aldrich. For MALDI-TOF/MS analysis, 2,5-dihydroxybenzoic acid (Wako, Osaka, Japan) was used as a matrix. The water used for all experiments was purified using a MilliQ UV plus water purification system (Millipore, Bedford, MA). Sequencing-grade unmodified trypsin, Glu-C and Asp-N were obtained from Roche Diagnostics (Mannheim,